Modeling greenhouse gas emissions from riverine systems: a review

Diego G. Panique-Casso[1]*, Peter Goethals[1], Long Ho[1]

[1] *Department of Animal Sciences and Aquatic Ecology, Ghent University, Ghent, Belgium.*

* Corresponding author. Email: Gustavo.PaniqueCasso@UGent.be

Abstract

Despite the recognized importance of flowing waters in global greenhouse gas (GHG) budgets, riverine GHG models remain oversimplified, consequently restraining the development of effective prediction for riverine GHG emissions feedbacks. Here we elucidate the state of the art of riverine GHG models by investigating 148 models from 122 papers published from 2010 to 2021. Our findings indicate that riverine GHG models have been mostly data-driven models (83%), while mechanistic and hybrid models were uncommonly applied (12% and 5%, respectively). Overall, riverine GHG models were mainly used to explain relationships between GHG emissions and biochemical factors, while the role of hydrological, geomorphic, land use and cover factors remains missing. The development of complex and advanced models has been limited by data scarcity issues; hence, efforts should focus on developing affordable automatic monitoring methods to improve data quality and quantity. For future research, we request for basin-scale studies explaining river and land-surface interactions for which hybrid models are recommended given their flexibility. Such a holistic understanding of GHG dynamics would facilitate scaling-up efforts, thereby reducing uncertainties in global GHG estimates. Lastly, we propose an application framework for model selection based on three main criteria, including model purpose, model scale and the spatiotemporal characteristics of GHG data, by which optimal models can be applied in various study conditions.

Keywords: Greenhouse gas, river, stream, driving factor, modeling

List of acronyms

A: Watershed area

Chl-a: Chlorophyll a

C_{CO2}: CO_2 concentration

C_{CO2gw}: CO_2 molarity in the groundwater

C_{CO2atm}: CO_2 molarity in the atmosphere

C_{NO3}: Nitrate concentration

C_{N2O_rip}: Nitrite concentration in the riparian zone

C_{N2O_soil}: Nitrite concentration in the soil area

CI: Confidence interval

d_{50}: Median grain size of streambed sediments

D or h or z: River depth

Dif: Diffusion coefficient

Disp: Dispersion coefficient

DO: Dissolved oxygen

DOC: Dissolved organic carbon

DIC: Dissolved inorganic carbon

DIN: Dissolved inorganic nitrogen

ER: Emission rate

EcoR: Ecosystem respiration

F*N_2O: N_2O emission flux

F_{WC}: Molar flux of CO_2 from water column

F_{he}: Molar flux of CO_2 from hyporheic zone respiration

g: Gravity force

GPP: Gross primary production

K_{600}: Gas exchange rate normalized to a Schmidt number of 600

K_{CO2}: Reaeration coefficient of CO_2

K_h: Stream hydraulic conductivity

K_{NIT}: Rate constant for nitrification

L_{st}: Stream length

L_{DIN}: DIN load

MF: Methane formation

NPP: Net primary production

NO_2: Nitrite

NO_3: Nitrate

NH_4: Ammonium

OM: Organic matter

PPFD: Photosynthetic photon flux density

Pop_Density: Population density

P_{N2O_denrip}: Rate of production of N_2O

pCO_2: Particulate CO_2

Q: Discharge

$R_{autotrophic}$: River autotrophic respiration

$R_{heterotrophic}$: River heterotrophic respiration

$R_{hyporheic}$: River hyporheic respiration

S_o: Average slope gradient

SIM: Suspended inorganic matter

SOM: Suspended organic matter

SSS: Sea surface salinity

SST: Sea surface temperature

t_m: Time of turbulent vertical mixing

T_{air}: Air temperature

T_w: Water temperature

TCG: Total carbon gas concentration ($CO_2 + CH_4$)

TN: Total nitrogen

TP: Total phosphorous

V or u: River velocity

V_{fden}: Uptake rate of denitrification

W or B: River width

Y_{DIN}: DIN yield

∅1: Arrhenius coefficient

α_{ox}: Water column methane oxidation rate

τ_{50}: Median hyporheic residence time

τ_D: Time of denitrification

1. Introduction

Rivers have recently become recognized as an important component of the carbon (C) cycle and represent a potential yet-to-be-quantified feedback of climate change. Global estimates of riverine CO_2 emissions range from 0.65 (95% CI: 0.48–0.84) to 2.0 ± 0.2 Pg CO_2 yr^{-1} (Lauerwald et al., 2015; Liu et al., 2022), equivalent to 33.7% of total anthropogenic emissions from industrial activities and land use change (Drake et al., 2018) and higher than the annual terrestrial carbon sink of 3.6 Pg C yr^{-1} (Keenan and Williams, 2018). Riverine CH_4 emissions range from 1.5 to 26.8 (5^{th}–95^{th} percentiles: 0.01–160) Tg CH_4 yr^{-1} (Bastviken et al., 2011; Stanley et al., 2016) equivalent to 15–40% of the emissions from wetlands and lakes combined (Stanley et al., 2016). And riverine N_2O emissions range from 72.8 to 291.3 ± 58.6 Gg N_2O yr^{-1} (Marzadri et al., 2021; Yao et al., 2020), about 1–10% of the global anthropogenic N_2O emissions (Beaulieu et al., 2011; Tian et al., 2020). Significant discrepancies within GHG estimates are reported because of the use of different estimation methods or models, which use datasets with varying characteristics, different data processing techniques, and include diverse assumptions such as the inclusion or exclusion of headwaters in global assessments (Beaulieu et al., 2011; Lauerwald et al., 2015; Marzadri et al., 2021; Rosentreter et al., 2021; Yao et al., 2020). As such, the real potential of riverine systems to contribute to GHG emissions is yet unquantified.

By excluding the complexity of riverine ecosystems, current estimation models of riverine emissions are oversimplified with questionable assumptions, hence have been reported to be error-prone. For example, emission factors (EF) assume that emissions are proportional to nitrogen (N) inputs (IPCC, 2019, 2006), while upscaling techniques assume that regional fluxes are proportional to point measurements, surface area, and local gas transfer velocities (Bastviken et al., 2011; Cole et al., 2007; Raymond et al., 2013). These oversimplified methods disregard multiple essential drivers, such as land use and cover (LULC) or lateral fluxes, consequently causing errors in estimation of as high as 42% (Yang et al., 2022). To improve the estimation of riverine GHG emission, several modeling approaches have been proposed lately, offering diverse methodologies and knowledge frameworks. However, no review of the models for riverine GHG emissions can be found to analyze their current status, identify challenges and limitations, and guide future developments in this field.

In contrast to recent reviews that provide an overview of methods to achieve global-scale estimates (Lauerwald et al., 2023) or focus on GHG emissions modeling in lentic waters (Ion and Ene, 2021; Levasseur et al., 2021), this review centers on critically evaluating the state of the art of riverine GHG models across diverse case studies with varied spatiotemporal scales. As such, we conducted a comprehensive analysis of 148 models obtained from 122 publications published over the past 11 years (2010–2021). The goal of this review is threefold: 1) to provide new insights into the potential challenges and issues associated with existing models; 2) to define their role in quantifying regional and global GHG budget; and 3) to guide future development of modeling techniques. This review

focuses on diverse elements of model selection and development, which are progressively scrutinized in three sections. First, we define the three model types and elucidate their properties, advantages, and disadvantages. Second, we characterize these models according to model purposes, model scales, data attributes, modeled factors, and uncertainty analysis. These findings are mapped into a decision tree to facilitate model selection for future studies, considering specific requirements and objectives of researchers. Finally, we critically discuss challenges associated with riverine GHG models and highlight key research needs and future directions to enhance the accuracy and reliability of these models.

2. Methodology

To investigate recent studies on riverine GHG emission modeling, we launched a detailed review of the studies published in peer-reviewed journals on the Scopus platform for the timeframe 2010–2021 by applying the query TITLE (river* AND (nitrous* OR "carbon dioxide*" OR "greenhouse gas*" OR CO_2 OR methan* OR CH_4 OR N_2O)) AND PUBYEAR > 2009 AND PUBYEAR < 2022 AND TITLE-ABS-KEY (model* OR method* OR framework* OR estim* OR predict*). In total, 707 publications were collected. We scrutinized these studies by eliminating publications on unrelated topics, ultimately obtaining 122 relevant publications, including 148 models almost equally distributed among the main GHGs: CO_2 (40%), CH_4 (29%) and N_2O (31%) (Figure S1 in supplementary material). The studies collected were used to investigate factors of interest, including model types, model purposes, model scales, riverine GHG data attributes, modeled factors, and uncertainty analysis. Based on modeling paradigm, we identified three model types: data-driven, mechanistic, and hybrid models (Figure S2), which, according to their purpose, were subcategorized into explicative and predictive models. Given their scale of application, these models were subclassified into site-, basin-, or global-scale models. Similarly, we investigated data attributes that are used for model development by identifying data collection methods, sampling frequency, and sampling duration. Additionally, we determined driving factors that are commonly used as inputs in riverine GHG models, namely biochemical, hydrological, geomorphic factors, and LULC types. This subclassification of factors is described in Table S3. Finally, we evaluated the use of uncertainty analysis and model validation techniques in riverine GHG models. Note that these characteristics were selected to represent main steps in model selection and development, which can enable us to define the state of the art of riverine GHG models. It is worth mentioning that we excluded the boundary layer method to estimate fluxes via gas exchange as this method was out of scope of our review and was thoroughly investigated in Hall Jr. and Ulseth (2020).

3. Model types

Illustrating the distribution of model types from 2010 to 2021, Figure 1A reveals that the majority of riverine GHG models have been data-driven models (83%), while mechanistic and hybrid models have

been constructed less frequently (12% and 5%, respectively). Prior to 2015, all riverine GHG models were data-driven, with less than 10 models published per year. However, since 2015, there has been a considerable increase in the number of models, reaching a peak of 34 models in 2021, with a breakdown of 10 models for CO_2, 15 for N_2O, and 9 for CH_4. This increase is accompanied by the growing application of mechanistic and hybrid models, which implies a better understanding of the mechanism and production pathways of riverine GHG dynamics. GHG modeling studies were mainly developed in highly industrialized countries such as China and United States that concentrate ~60% of riverine modeling research (Figure 1B). While tropical areas are missing, especially in Africa and South and Central America, which might be significant given the high concentrations of GHGs reported in these waters (Aufdenkampe et al., 2011).To further shed light on the current state of riverine GHG models, a detailed analysis of the specific characteristics of these models is provided in the following section.

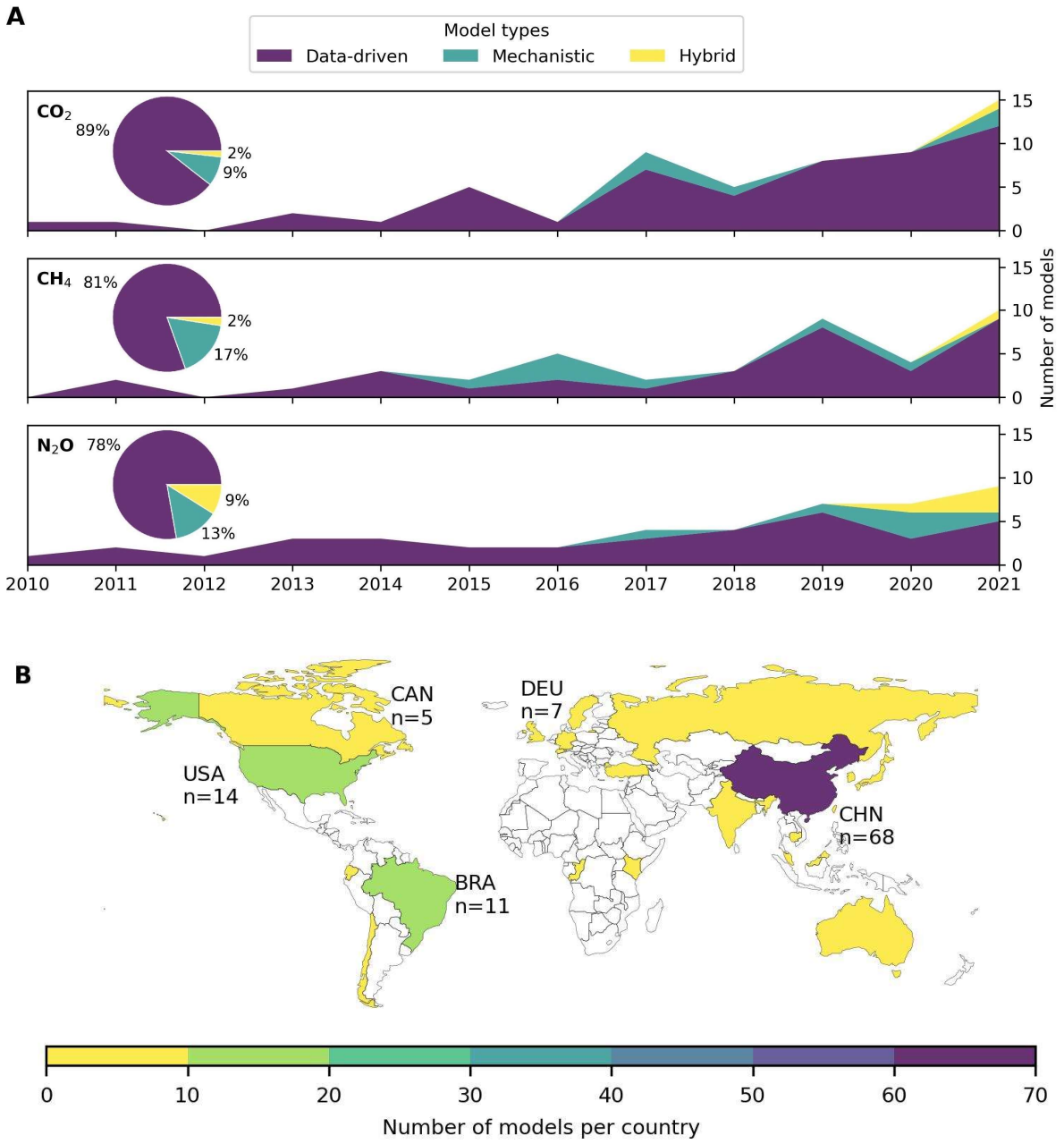

Figure 1. Chronological evolution (A) and spatial distribution (B) in the development of riverine GHG models, including the number of modeling studies in the top-five countries (CHN: China, USA: United States of America, BRA: Brazil, DEU: Germany, CAN: Canada).

3.1. Data-driven models

Data-driven models rely on observed data to define relationships between GHG fluxes or concentrations with driving factors. In our review, we found that these relationships are mainly defined statistically by applying methods such as principal component analysis (PCA) and regression analysis, or empirically with EFs and upscaling techniques, while other data-driven methods such as non-linear models have been scarcely applied (Figure S2). The differences between these main approaches is in their model structure and purpose. Statistical models can adapt model structure to collected data in order to obtain

optimal relationships and model performance, while empirical models have their structure fixed. Due to this flexibility, statistical models can be used to explore raw data and identify relationships between model inputs and output (Begum et al., 2021; Xiao et al., 2021). On the other hand, empirical models assume that GHG emissions are proportional to point measurements in the system. As such, values of EFs are used to transform N inputs into N_2O emissions and GHG point measurements are converted to regional and global emissions by multiplying them with surface area and gas transfer velocities (Aufdenkampe et al., 2011; Hu et al., 2016). Note that, given the diverse conditions of river systems, different equations of EFs have been obtained to estimate riverine N_2O emissions with diverse characteristics, such as hydrogeological conditions (Cooper et al., 2017) or climate (Hu et al., 2016).

Data-driven models have been applied for modeling site-scale riverine emissions, taking mainly into account biochemical processes (Table 1 and Figure S3). For instance, CO_2 data-driven models have focused on chemical equilibria of aquatic inorganic carbon – as such, pH, OC, DO, and Chl-a variables are included – while CH_4 and N_2O models have accounted for microbial processes, thereby using different forms of nutrients. Data-driven models are preferred due to their flexibility. Even with limited datasets, these models can provide initial insights and practical predictions, which can be valuable for making informed decisions or guiding further data collection efforts (Gu et al., 2021). However, the performance of data-driven models heavily relies on quality, quantity, and representativity of data. Therefore, the captured relationships are strongly dependent on the characteristics of collected data. Specifically, in riverine research, sampling campaigns have been conducted often under different climatic conditions, locations, seasons, and sampling periods, consequently, leading to datasets and models containing distinct characteristics (Xia et al., 2014). Moreover, the experimental design, such as sampling methods and measurement techniques, introduce further variation in data (Bastviken et al., 2022). Due to this strong dependence on datasets, data-driven models are limited to provide general comprehensive results, and their ability to make predictions beyond the observed data is restricted.

Table 1. Summary of the data-driven models riverine GHG models encountered in this review. ns: not specified.

System	Equation	R^2	Reference
Regression analyses			
CO_2			
Amazon Estuary, Brazil	$pCO_2 = 0.05*SSS^2 + 34.81*SST^2 + 19.71*SSS*SST + 48792.07 – 560.47*SSS – 2694.56*SST$	0.74	Valerio et al. (2021)
River Kelvin, UK	$F_{CO2} = 1.01*Q + 0.17$ $pCO_2 = 0.09*Q – 0.10$	0.64 0.96	Gu et al. (2021)
Upper Yangtze River, China	For the Taohua river $pCO_2 = –3637*pH + 280*DOC + 30587$	0.84	Tang et al. (2021)
	For the Nan river $pCO_2 = –1341*pH + 12640$	0.40	

	For the Puli river pCO_2 = –2535*pH + 392*Chl-a + 21896	0.78	
	For winter season pCO_2 = –2712*pH + 308*DOC + 22810	0.87	
	For summer season pCO_2 = –3022*pH + 214*Chl-a + 26165	0.83	
	For all seasons pCO_2 = –3092*pH + 130Chl-a + 46*CFU + 26704	0.85	
Tanswei River, Northern Taiwan	pCO_2 = 1.88*turbidity + 10160.507*SOM + 71.930*SIM – 46.157*NO_3 + 3705.831	ns	Yang et al. (2015)
Global	Log(pCO_2) = –3.192 + 9.372*Pop_density – 0.279*log(S_o) + 1.343*T_{air} + 0.279*NPP	0.47	Lauerwald et al. (2015)
Boreal River	Log(pCO_2) = –2.76 + 0.28*Log(DOC) – 0.22*Log(V)	0.38	Campeau and Del Giorgio (2014)
CH_4			
Upper Yangtze River, China	When urban land proportion < 2% pCH_4 = 8493 – 973*pH	0.27	Tang et al. (2021)
	When 2% ≤ Urban land proportion < 20% pCH_4 = 1430 + 929*TN – 27*DO – 388*Chl-a + 3620*TP	0.75	
	When 20% ≤ Urban land proportion ≤ 46% pCH_4 = 7191 + 3498*TN – 8598*NO_3	0.96	
	For all land use types pCH_4 = 1679 + 1411*TN – 10153*NH_4 + 9432*TP – 708*NO_3	0.59	
River Kelvin, UK	F_{CH_4} = 2.53*Q + 3.70 pCH_4 = 0.17*Q – 0.17	0.46 0.91	Gu et al. (2021)
Flooding event Indigirka River, Siberia	pCH_4 = –1.90*(reflectance) + 1.02	0.94	Morozumi et al. (2019)
Tanswei River, Northern Taiwan	pCH_4 = 84.463*SIM + 864.274*NH_4 – 456.171	ns	Yang et al. (2015)
Boreal River in Québec, Canada	Log(CH_4)/TCG = –2.90 + 0.06*T_w	0.39	Campeau and Del Giorgio (2014)
N_2O			
Saitama, Japan	pN_2O = 0.34*NO_2-0.30*pH + 0.22*NH_4 + 0.26*NO_3 + 0.23*DOC	0.64	Mishima et al. (2021)
Xiaoyue River, China	FN_2O = 4810.3$e^{-0.26*DO}$	0.70	Wang et al. (2020)
Mara River, Kenya	When forest land use proportion > 70% pN_2O = 0.23 + 0.10*pCO_2 + 1.71*NH_4 – 0.03*DOC	0.59	Mwanake et al. (2019)

	When agricultural land use proportion > 70% $pN_2O = 1.49 + 0.27*pCO_2 – 0.18*DO – 0.05*DOC$	0.77	
	When livestock land use proportion > 70% $pN_2O = 1.52 – 0.42*pCO_2 – 0.22*DO$	0.45	
Changjiang River estuary, China	$pN_2O = f(NO_3)*Q$ $Log(N_2O) = –0.39 + 0.69*Log(NO_3)$	0.52	Yan et al. (2012)
Empirical models			
CO_2			
Global	$F_{CO_2} = \sum A*k*pCO_2$ $F_{CO_2} = \sum A*F_{CO_2}$		Aufdenkampe et al. (2011)
CH_4			
Global	$F_{CO_2} = \sum A*F_{CH_4}$		Stanley et al. (2016)
N_2O			
Global	For freshwater systems EF_{5r} = 0.0026 (kg N_2O per kg of N inputs to rivers) $EF_{5r} = N_2O/NO_3$		IPCC (2019)
Rivers Avon, Eden, and Wensum, UK	For unconfined chalk hydrogeological conditions EF_{5r} = 0.00036; $EF_{5r} = N_2O/NO_3$		Cooper et al. (2017)
	For semi-confined chalk hydrogeological conditions EF_{5r} = 0.00020; $EF_{5r} = N_2O/NO_3$		
	For confined chalk hydrogeological conditions EF_{5r} = 0.00016; $EF_{5r} = N_2O/NO_3$		
Global	General equations $ER_{N_2O} = 0.0034*Y_{DIN}^{-0.169}$ $L_{DIN} = 0.0034*Y_{DIN}^{0.831}*A$ $ER_{N_2O} = 0.0138*Y_{DIN}^{-0.417}$ $L_{DIN} = 0.0138*Y_{DIN}^{0.583}*A$		Hu et al. (2016)
	For subtropical and tropical rivers $ER_{N_2O} = 0.0044*Y_{DIN}^{-0.179}$ $L_{DIN} = 0.0044*Y_{DIN}^{0.821}*A$ $ER_{N_2O} = 0.0112*Y_{DIN}^{-0.355}$ $L_{DIN} = 0.0112*Y_{DIN}^{0.645}*A$		
	For temperate rivers $ER_{N_2O} = 0.0041*Y_{DIN}^{-0.230}$ $L_{DIN} = 0.0041*Y_{DIN}^{0.770}*A$ $ER_{N_2O} = 0.0198*Y_{DIN}^{-0.521}$ $L_{DIN} = 0.0198*Y_{DIN}^{0.479}*A$		

3.2. Mechanistic models

Based on model structure and complexity, three types of mechanistic models are observed: conceptual, mass-balance biochemical, and mass-balance hydraulic models (Table 2). Conceptual models apply simplified forms of physical or chemical principles to define relationships between GHG fluxes or concentrations with driving factors. For instance, Marzadri et al. (2017) estimated N_2O emissions at a

basin scale, based on two denitrification Damköhler numbers, Da_{DHZ} and Da_{DS}. The first model accounts for emissions from streams where hyporheic and benthic processes play an important role, while the second simulates emissions from rivers where processes in the water column are more important. Mass-balance biochemical models are usually one-dimensional models that estimate the time-variant transformation of C and N sources into riverine GHGs. For example, Newcomer et al. (2018) applied a mass-balance model to study nutrient transformation in the hyporheic zone, including storage and release of C and N in biomass and biogenic CO_2 and N_2 to the atmosphere, driven by fluctuations in groundwater levels, antecedent hydrological conditions, riverbed sediment characteristics, and DOC delivery.. Mass-balance hydraulic models are two-dimensional models that simulate the spatial- and time-variant concentration of C and N components along the river network, including transformation processes in the water column and the interaction of these with lateral sources. Mass-balance hydraulic models include two major modules: flow and reactive transport. The flow module simulates the propagation of flow in a channel, while the reactive transport module simulates the quantity and fate of GHG components using transport coefficients, such as diffusion and dispersion (Akella and Bhallamudi, 2019). Mass-balance hydraulic models are particularly useful to evaluate interactions of C and N components carried by the river with groundwater inputs and point effluents at different locations, thereby providing a detailed modeling framework for predicting hotspots of GHG emission and production (Saccardi and Winnick, 2021).

Mechanistic models use fundamental knowledge to describe via mathematical expressions and physical principles, temporal and/or spatial changes in C, N, and resulting GHG components. Mechanistic models are more comprehensive than data-driven models, being suitable to provide new insights into system processes and mechanisms and extrapolate beyond observed data (Pfeiffer-Herbert et al., 2019). However, the extensive system representativity of mechanistic models can lead to complex calculations and overparameterization, which increases substantially required data (Ho et al., 2019). As a result, river modelers often appeal to certain assumptions on model parameters and boundary conditions, such as denitrification conversion ratio or zero initial GHG concentrations (Saccardi and Winnick, 2021; Stets et al., 2017; Vanderborght et al., 2002). These assumptions often distort the representation of the real system, introducing biases into modeling results.

Table 2. Summary of the mechanistic riverine GHG models encountered in this review.

System	Equation	Reference
Conceptual models		
N_2O		
Upper Mississippi River basin, USA	$\sum_{i=1}^{NC} ER_{N2O,i} = \sum_{i=1}^{NC} V*DIN_i * F^*N_2O*W_i * L_{St,i}$ When river width ≤ 10 m $F^*N_2O_{HZ} = 1.55*10^{-7}*(Da_{DHZ})^{0.43}$	Marzadri et al. (2020, 2017)

	When 10 m < river width ≤ 175 m $F^*N_2O_{BZ} = 1.91*10^{-8}*(Da_{DHZ})^{0.58}$	
	When river width W > 175 m $F^*N_2O_{WC} = 4.56*10^{-6}*(Da_{DS})^{0.72}$	
	$Da_{DHZ} = \tau_{50}/\tau_D = 17.810*g*D*V_{fden}/(K_h*V^2)$	
	$Da_{DS} = t_m/\tau_D = 14.925*V_{fden}/(g*D*S_o)^{1/2}$	
CH_4		
Saar River, Germany	$MF_{Z_1T}=\left(a_1*e^{-\frac{z}{z_1}}+a_2*e^{-\frac{z}{z_2}}+a_3\left(\frac{1}{1+e^{-b_3z_3+c_1}}-1\right)\right)a_4T^{b_4}$	Wilkinson et al. (2015)
Mass-balance biochemical models		
CO_2		
Connecticut River, USA	$\Delta DO_{i,d}=\left(\frac{GPP_d}{D_{i,d}}\times\frac{PPFD_{i,d}}{\overline{PPFD_d}}\right)+\left[\left(\frac{EcoR_d}{D_{i,d}}\right)+f_{i,d}(K_{600d})(DOsat_{i,d}-DO_{i,d})\right]\times\Delta t$ $DIC_t = DIC_{t-1} - K_{CO2}*(CO_{2,t-1} - CO_{2,sat}) - GPP_{DIC,t-1} + EcoR_{DIC,t-1}$	Aho et al. (2021)
Russian River, USA	$\frac{dCO_2}{dt} = GPP - R_{autotrophic} - R_{heterotrophic} + R_{hyporheic} \pm Dif$	Newcomer et al. (2018)
N_2O		
Seine River, France	$P_{N2O\_denrip} = \frac{N_2O}{N_2O+N_2}*\Delta C_{NO3\_denrip}*Q$ $Q \times C_{N2O\_rip} = Q\times C_{N2O\_soil} + P_{N2O\_denrip} + kvs \times A_{rip}\times (C_{N2O\_soil} - C_{eq}) - kvs \times A_{rip}*(C_{N2O\_rip} - C_{eq})$	Billen et al. (2020)
CH_4		
Cambridge Bay estuary, Canada	$C_{CH4_{t+1}} = (C_{CH4_t}V_{box} + F_{riv,t} + F_{ice,t} + F_{gasex,t} + F_{in,t} + F_{out,t} + F_{ox,t})/V_{box}$ $F_{riv,t} = V_{riv,t}*C_{CH4\_riv,n,t}$ $F_{ice,t} = V_{ice,t}*C_{CH4\_ice,n,t}$ $F_{in,t} = (V_{riv,t} + V_{ice,t})*C_{CH4,n-1,t-1}$ $F_{out,t} = -(V_{riv,t} + V_{ice,t})*C_{CH4,n,t}$ $F_{gasex,t} = K_{CH4,t}(C_{CH4,eq,t} + C_{CH4,n,t})*V_{box}*dt$ $F_{ox,t} = -K_{ox,t}*C_{CH4,t}*V_{box}*dt$	Manning et al. (2020)
Mass-balance hydraulic models		
CO_2		
East River, USA	$\frac{dC_{CO2}}{dt} = -V\frac{dC_{CO2}}{dx} + \frac{1}{A}\frac{dQ}{dx}(C_{CO2gw} - C_{CO2}) - k_{CO_2}(C_{CO2} - C_{CO2atm}) + F_{wc} + F_{he}$	Saccardi and Winnick, (2021)
N_2O		
Tyne River, UK	$\frac{\partial D}{\partial t} + D\frac{\partial V}{\partial x} + V\frac{\partial D}{\partial x} + \frac{D*V}{W}\frac{dW}{dx} = \frac{Q_L}{W*\Delta x}$	Akella and Bhallamudi (2019)

	$\frac{\partial NH_4}{\partial t} + V\frac{\partial NH_4}{\partial t} = \frac{1}{A}\frac{\partial}{\partial x}\left(A*Disp_x\frac{\partial NH_4}{\partial x}\right) + \left(\frac{Q_L}{A}\right)NH_{4Lat} + \frac{R_{Ammon}}{h} - K_{NIT}NH_4\emptyset_1^{T-20} - K_{Alg\text{-}up}NH_4$ $\frac{\partial NO_3}{\partial t} + V\frac{\partial NO_3}{\partial t} = \frac{1}{A}\frac{\partial}{\partial x}\left(A*Disp_x\frac{\partial NO_3}{\partial x}\right) + \left(\frac{Q_L}{A}\right)NO_{3Lat} - K_{NIT}NO_3\emptyset_1^{T-20}$ $\frac{\partial N_2O}{\partial t} + V\frac{\partial N_2O}{\partial t} = \frac{1}{A}\frac{\partial}{\partial x}\left(A*Disp_x\frac{\partial N_2O}{\partial x}\right) + \left(\frac{Q_L}{A}\right)N_2O_{Lat} + \frac{0.25}{100}* K_{NIT}*N_2O*\emptyset_1^{T-20} - \alpha(N_2O - N_2O_{atm})$	
CH_4		
Columbia River, USA	$Q_{j,k} = V_{j,k}*\Delta y*\Delta z$ $A\frac{\partial C_{CH4}}{\partial t} = \frac{\partial}{\partial x}\left[Q_R C_{CH4} + A*Dif_H\frac{\partial C_{CH4}}{\partial x}\right] + A*\left[\frac{K_{CH4}}{H}\left(C_{CH4_{sat}} - C_{CH4}\right) - \alpha_{OX}C_{CH4} + CH_{4Lat}\right]$	Pfeiffer-Herbert et al. (2016)

3.3. Hybrid models

Hybrid models combine data-driven models and mechanistic models to leverage their strengths and potentially provide more comprehensive and accurate assessments. This model type is able to integrate diverse knowledge realms, data sources, and formats into its calculations, thereby providing a holistic analysis of the system (Jia et al., 2020). A holistic approach is highly required in riverine GHG research, as land-surface and riverine processes need to be integrated to simulate the entire cycle of GHG dynamics and accurately estimate the fate and transport of C, N, and GHG components (Borges et al., 2015).

Table 3 shows hybrid models collected in this review. What is noticeable is the flexibility of this model type, as a data-driven model can be used to either complement the outputs of a mechanistic model or provide input variables. This characteristic is particularly useful in riverine GHG research as well-established mechanistic models can be used to simulate processes such as C and N biogeochemical transformations in the river (Ho et al., 2021) or hydrology driving the transport of C and N components from land-surface to riverine systems (Gao et al., 2020). In the meantime, a data-driven model can be used to predict riverine GHG emissions from the outputs of a mechanistic model, thereby providing a holistic approach of the cycling of water, C, N, and GHGs. Additionally, data-driven models can also provide inputs for a mechanistic GHG model, thereby creating tools to estimate global N_2O emissions (Marzadri et al., 2021).

Despite these advantages, hybrid models face challenges that hinder their application. These challenges include complexity, specialized knowledge requirements, discrepancies in temporal and spatial scales of models, and concerns regarding the interpretability of their outcomes (Kratzert et al., 2019). Integrating diverse data sources and model types demands for substantial computational resources and expertise, posing time and cost barriers (Willard et al., 2020). Moreover, the accuracy and interpretability of hybrid models remains disputed, as these models usually rely on physical constraints of mechanistic components to provide transparency to their calculations, which might be unrealistic or

insufficient to explain model output (Chen et al., 2022). Furthermore, the lack of interpretative tools to validate the accuracy of hybrid models contributes to their characterization as black-box models (Schneider et al., 2022).

Table 3. Description of the hybrid riverine GHG models encountered in this review.

System	Model 1	Model 2	Reference
CO_2, CH_4, and N_2O			
Cuenca River basin, Ecuador	Mechanistic model: River Water Quality Model No.1 (RWQM1) and Activated Sludge Model No.1 (ASM1)	Data-driven model: fuzzy models to evaluate risk of GHG accumulation in the river	Ho et al. (2021)
N_2O			
Naoli River basin, China	Mechanistic SWAT hydrological model	Data-driven N_2O regression model	Gao et al. (2020)
Global	Data-driven models to calculate hydrological and morphological factors: W, D, V, S, d_{50}, K_h, L_{st}, V_{fden}, τ_{50}, τ_D, t_m	Mechanistic N_2O emission model	Marzadri et al. (2021)
Manistee and Tippecanoe River basins, USA	Data-driven models to calculate hydrological and morphological factors: W, D, V, S, d_{50}, K_h, L_{st}, V_{fden}, τ_{50}, τ_D, t_m	Mechanistic N_2O emission model	Tonina et al. (2021)

4. Current status of riverine GHG models

4.1. Model purposes

Regarding model purposes, riverine GHG models can be classified into explicative or predictive (Figure 2). Explicative models aim to explain the relationships and underlying mechanisms between driving factors of GHGs. Examples include statistical causal analyses, such as multiple linear regressions (Hao et al., 2021) and PCA analyses (Shen et al., 2020), and mechanistic models that validate the hypothesis of GHG dynamics (Pfeiffer-Herbert et al., 2016). Predictive models, on the other hand, forecast the value of GHG concentrations or fluxes based on the status of driving factors. Their focus is to develop models that can extrapolate precisely to unseen data. Examples include regression models used to forecast global CO_2 emissions using changes in basin population density, slope of the river, air temperature, and net primary production (Lauerwald et al., 2015), or mechanistic models used to simulate scenarios to determine the optimal allocation of wastewater effluents in tidal rivers (Akella and Bhallamudi, 2019). Note that studies also combined explicative and predictive techniques, such as PCA to determine the principal drivers of GHG production, followed by regression models that use these factors for prediction (Tang et al., 2021).

Figure 2 shows that explicative models are more commonly applied than predictive models, reflecting the ongoing interest of researchers in understanding the causal relationships between driving factors

and GHG emissions. Among explicative models, the data-driven approach prevails in CO_2 (76%), CH_4 (68%) and N_2O (58%) models, followed by much fewer applications of mechanistic models at 7%, 16% and 4% in CO_2, CH_4 and N_2O, respectively. Predictive models also show a dominance of data-driven approaches (13%, 14% and 20%), while mechanistic (2%, 0% and 9%) and hybrid models (2%, 2% and 9%) are less commonly applied. This data reveals the researcher preference for applying data-driven models, likely due to less data requirements, and for predicting N_2O emissions, which might be explained by the early concern over anthropogenic N inputs to river systems (Baulch et al., 2011; Seitzinger and Kroeze, 1998).

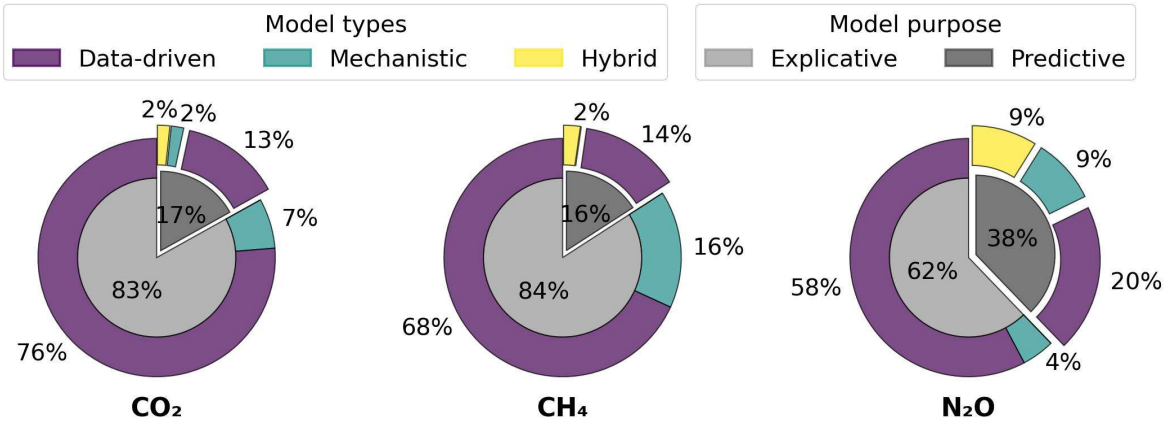

Figure 2. Description of riverine GHG models according to the model purpose.

4.2. Model scales

Riverine GHG modeling research is mostly applied at specific site-scale conditions, whereas the analysis of larger-scale systems (basin or global) is scarcely proposed (Figure 3). Site-scale studies apply either data-driven or mechanistic models, basin-scale studies apply either mechanistic or hybrid models, and global-scale studies apply data-driven, mechanistic, and hybrid models. This can be related to the distinct advantages that each model type offers at different scales.

Data-driven models are suitable either at the site or global scale. At the site scale, data-driven models excel at defining relationships between biochemical factors that locally affect GHG production and emissions. As shown in Section 3.1, multiple data-driven models are proposed to model chemical equilibria of aquatic inorganic carbon or microbial nutrient transformations. At the global scale, data-driven models are applied due to their flexibility in using datasets from heterogeneous systems without requiring to satisfy any physical constraint. Therefore, a single model can be applied simultaneously to multiple (and even ungaged) basins (Lauerwald et al., 2015). On the contrary, at the basin scale, data-driven models require extensive datasets because basin-scale processes are characterized by geomorphological heterogeneity and time-dependent relationships. For example, depending on antecedent hydrological conditions, such as accumulated precipitation and soil water content of the

basin before precipitation events, generated runoffs can either carry great soil CO_2 to a river triggering riverine emissions or conversely dilute CO_2 concentrations with rapid runoff to a river (Zhang et al., 2020). Since available riverine GHG datasets rarely satisfy this demand, more parsimonious mechanistic models are preferred for basin-scale practical applications.

Mechanistic models are able to simulate dynamics occurring at multiple temporal and spatial scales therefore being useful at any scale of analysis. At the site scale, these models provide detailed simulations of underlying physical and chemical processes, which allows researchers to understand processes where data is difficult to obtain. For example, mechanistic models were used to explain nitrification and denitrification processes in hyporheic zones, contributing to our understanding of the complexities of GHG fluxes (Hu et al., 2021). However, as the model size increases, required data and computational power also increase significantly. For instance, Yao et al. (2020) proposed a mechanistic model that integrates surface and subsurface hydrological and biogeochemical processes to estimate global riverine N_2O emissions. This model requires extensive data to define critical parameters, such as ratio of riverine N_2O production, thickness of the hyporheic zone, and surface area of streams and rivers, which are not available in global datasets, constituting great uncertainties in the model outcomes.

Contrary to data-driven and mechanistic models, hybrid models offer advantages across multiple scales by combining the strengths of different modeling approaches. They can integrate data-driven and mechanistic models to capture both site-scale biochemical processes and basin-scale land-surface processes. For instance, in Gao et al. (2020), the basin-scale model SWAT, originally designed to model hydrological, soil, and plant physiological processes, was complemented with a data-driven model to also account for biochemical riverine transformations of nutrients into N_2O fluxes. In other words, hybrid models offer the possibility of complementing well-established mechanistic basin-scale models, whose parameters and capabilities are largely investigated in the literature. Hybrid models are also applied at the global scale. For instance, Marzadri et al. (2021) designed data-driven models to derive parameters from globally available datasets that subsequently are inputted to mechanistic conceptual GHG models. Differently from fully data-driven global models, hybrid global models offer a knowledge-based background that explain, to a certain extent, the outcomes of the model. However, it must be noted that at the global scale, models oversimplify processes, likely omitting important sources and sinks of GHGs, such as wastewater inputs or drainages from urban and arable areas. Therefore, global models need to report uncertainties implied in their methodology (e.g., Yao et al., 2020).

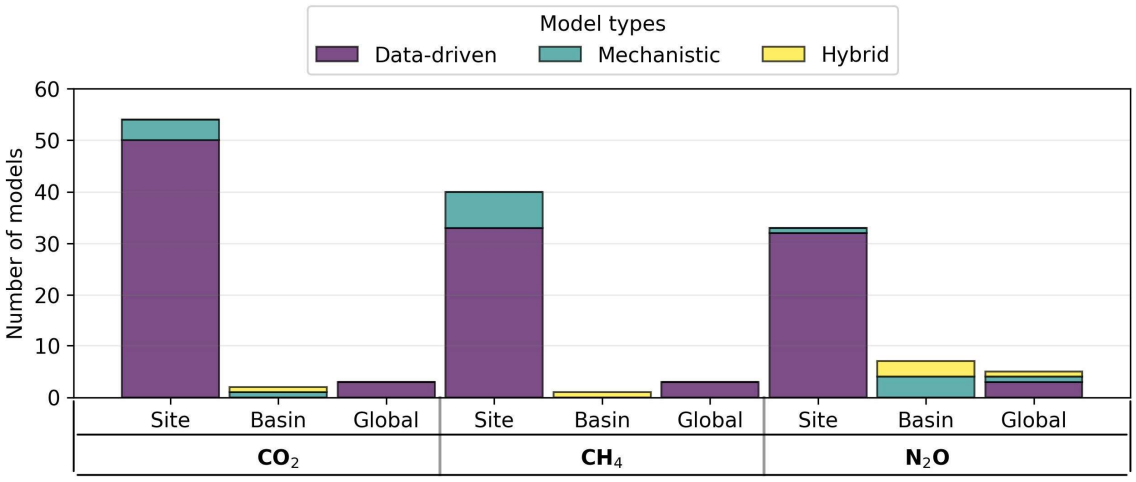

Figure 3. Characterization of the model scale of river GHG models. Site-scale models are applied locally to specific spots in the basin, while basin- and global-scale models combine data from multiple points into a single modeling framework.

4.3. Riverine GHG data attributes

The attributes of measurement methods and datasets used for riverine GHG model development is shown in Figure 4. The measurement methods are categorized based on data acquisition processes, namely indirect calculations and conventional and advanced measurements (Figure 4A). The first category uses chemical equilibria of aquatic inorganic C to calculate dissolved CO_2 concentration (pCO_2) (Nordstrom et al., 1979). Typical calculations of pCO_2 include the DIC-pH-temperature method (Abril et al., 2015; Hunt et al., 2011), the alkalinity-pH-temperature method (Hunt et al., 2011; Li et al., 2013; Liu et al., 2020) as well as software tools like CO2SYS (Lewis and Wallace, 1998) or PHREEQC (Parkhurst and Appelo, 2013). Conventional measurements correspond to manual methods used to collect data at specific site spots, such as floating chambers, the headspace method, bubble traps, and gas analyzers. Advanced measurements encompass non-invasive techniques that cover larger areas compared to conventional methods, such as hydroacoustic surveys and remote sensing techniques. Further details on these methods can be found in Bastviken et al. (2022). It is important to note that remote sensing techniques, including satellite surveys, face challenges in directly measuring GHGs in riverine systems due to detection limits, sample frequencies, and spatial coverage (Palmer et al., 2018; Thorpe et al., 2017). Consequently, proxies for GHGs are identified, such as reflectance or surface water temperature, which are then utilized to indirectly predict riverine GHG concentrations and fluxes (Morozumi et al., 2019; Valerio et al., 2021; Wilkinson et al., 2019).

Figure 4A indicates that 84% of the models are based on conventional measurements, namely the headspace method (48%), floating chamber (21%), and gas analyzers (15%). The extensive use of the first two techniques can be attributed to their lower costs and easier deployment compared to expensive gas analyzers and time-consuming bubble traps (4%) (Bastviken et al., 2022; Wilkinson et al., 2015). In addition to conventional methods, indirect calculations are employed (10%) despite their

373 acknowledged systematic errors due to overestimation of pCO_2 in acidic, organic-rich freshwaters
374 (Abril et al., 2015; Hunt et al., 2011; Liu et al., 2020). Furthermore, it appears that riverine GHG models
375 barely use data collected from advanced methods, which might be related to the high costs of
376 hydroacoustic surveys and technical difficulties of satellite surveys in rivers.

377 The majority of riverine GHG models (77%) are based on data collected over a period longer than a
378 month (Figure 4C). The low frequency of sample collection can be attributed to the prevalence of
379 conventional manual methods, such as the headspace method and floating chambers (Figure 4A).
380 Although the headspace method is simple to perform, increased sampling frequency requires multiple
381 displacements of human resources to the study site, whereas combining this method with automated
382 water collection systems is problematic due to difficulties in preserving samples unaltered, e.g., issues
383 regarding degassing in the sampled bottle (Johnson et al., 2010). In addition to multiple displacements
384 to the field, floating chambers also require a significant amount of deployment time, making it labor-
385 intensive to collect samples at shorter intervals (Thanh Duc et al., 2020). The few studies that obtained
386 higher temporal resolutions (1–2 weeks or continuous) involved either dedicated efforts by researchers
387 using manual methods or the use of automated methods that combined gas analyzers (Figure 4C). The
388 limited frequency of GHG data collection poses significant challenges in establishing comprehensive
389 relationships between GHGs and the drivers that influence emissions at high temporal resolution (Xia
390 et al., 2014). For instance, sporadic precipitation events cause the interruption of aquatic metabolism
391 processes, therefore changing the diurnal variation of CO_2 emissions from rivers (Zhang et al., 2020).

392 Furthermore, GHG data are often of short duration (Figure 4B), which can be attributed to the
393 aforementioned challenges associated with costly deployment and equipment. Overall, more than 90%
394 of riverine GHG models were built based on a dataset of less than 4 years, with the majority (59%)
395 using a dataset of 1–2 years. The use of short-term datasets hampers the comprehensive investigation
396 of the long-term effects that driving factors have on riverine GHG emissions, which likely fails to
397 capture a full range of GHG emissions from riverine systems (Borges et al., 2015). For instance, the
398 identification of seasonal trends and patterns of riverine GHG emissions and other environmental
399 factors is unlikely to be revealed with the absence of long-term datasets (Ran et al., 2021).

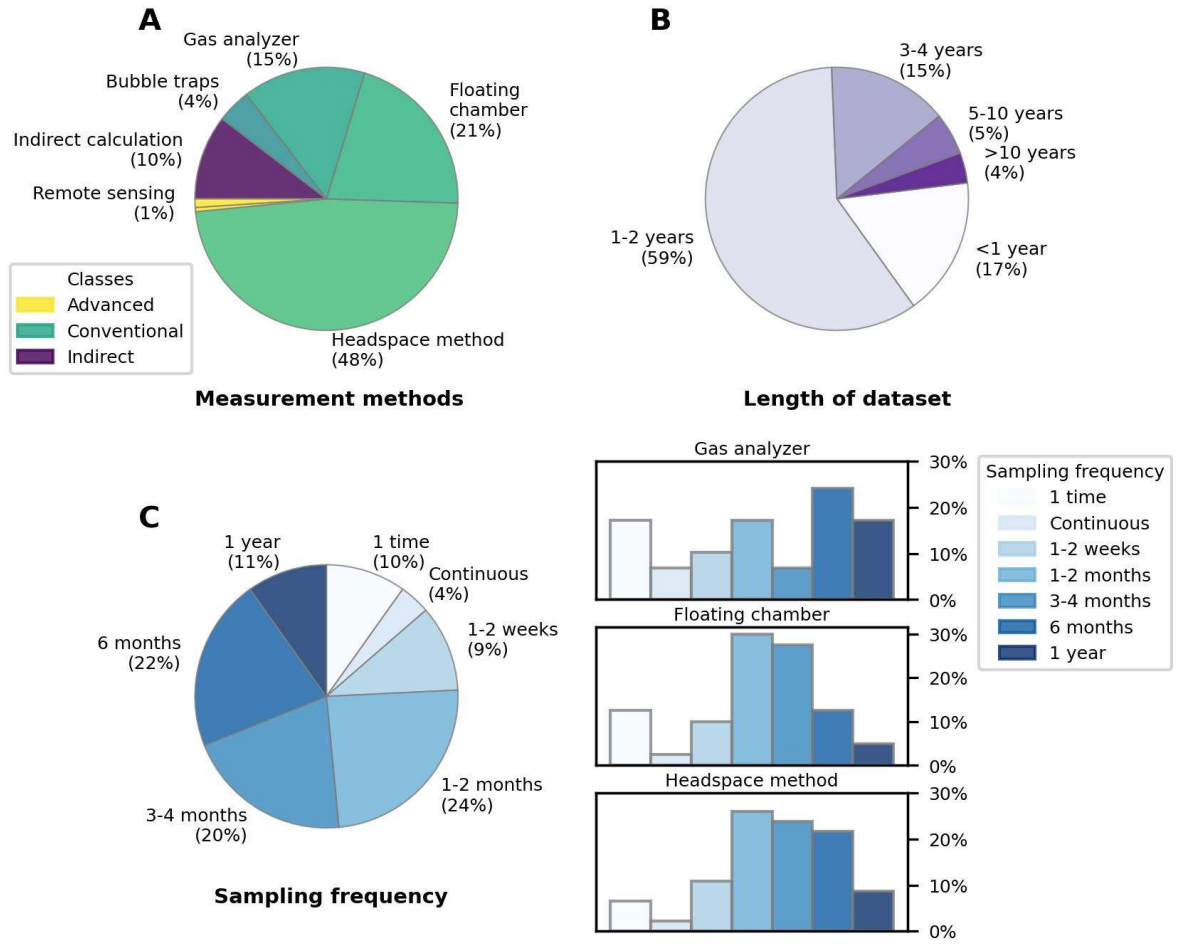

Figure 4. Percentage of riverine GHG models across distinct measurement methods (A), length of dataset (B), and sampling frequency (C). Figure C describes the sampling frequency of the three most frequently used measurement methods.

4.4. Modeled factors

This section elucidates the complexity of riverine GHG models by examining the number of factors that are incorporated in model development, namely biochemical, hydrological, geomorphic, and LULC factors (Figure 5). Integrating multiple factors is crucial in riverine GHG modeling, as overlapping effects of factors can create emission hotspots (Quick et al., 2019; Stanley et al., 2016). For instance, areas in which the river flows from low to high slopes can become emission hotspots as a result of OM accumulation, which is commonly driven by an increase in hydrological flow paths after precipitation events (Rocher-Ros et al., 2019).

Based on the number of modeled factors, the complexity of riverine GHG models increases from data-driven models to mechanistic and hybrid models (Figure 5). Data-driven models have incorporated one to four factors, focusing mostly on biochemical factors in contrast to infrequent use of hydrological,

geomorphic, and LULC factors. This degree of complexity of data-driven models remained steady from 2010 to 2021. On the other hand, mechanistic and hybrid models exhibit an increasing complexity by incorporating up to seven and eight factors, respectively. Although these models are able to integrate more hydrological and geomorphic factors, LULC factors have been rarely used.

The lack of integration of LULC factors might be explained by the difficulties in accurately representing this factor in existing models. LULC data is usually reported in maps where each grid is representative of a class or category (categorical spatial data). This troubles its integration with data-driven models that are based on point measurements (Mallast et al., 2020). For instance, LULC factors are currently represented into data-driven models simply as a percentage of the basin area, losing valuable spatial information through converting map details into numerical values (Tang et al., 2021). Contrarily, the mass-balance calculation scheme of mechanistic models allows the integration of LULC factors, but this can make the model and required data considerably more complex and lead to uncertain outcomes (Hu et al., 2021).

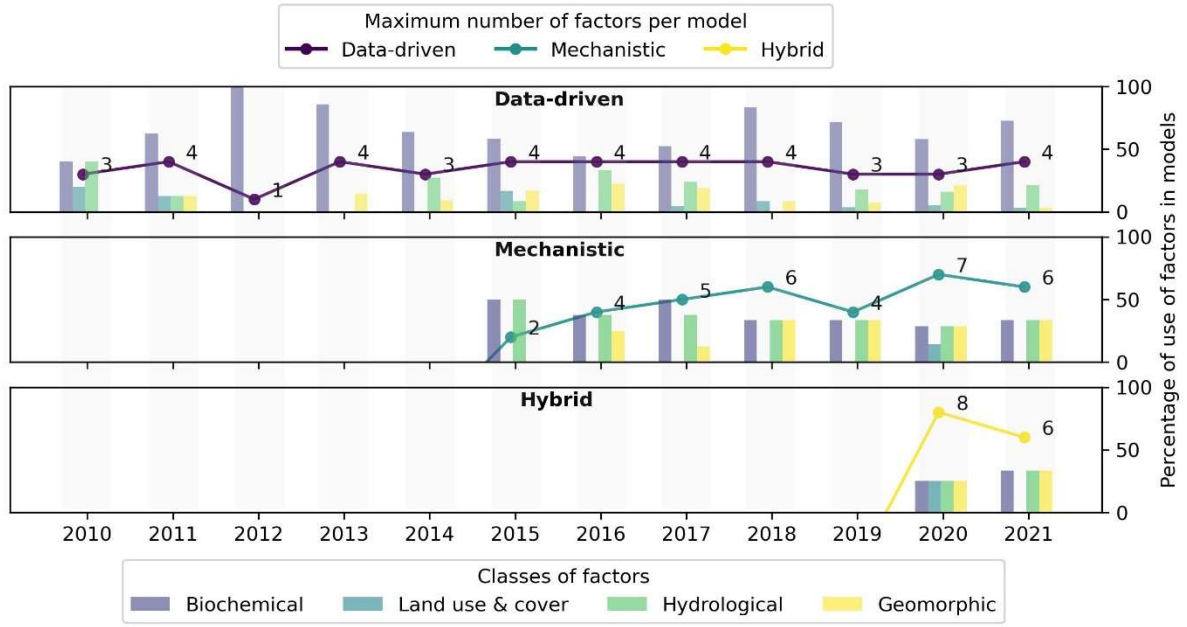

Figure 5. Description of model complexity across diverse model types. Line plots show the maximum number of factors used per year, while bar plots show the classes of these factors.

4.5. Uncertainty analysis

Reporting uncertainties associated with model outcomes is indispensable to increase the transparency of GHG emission inventories, thereby enabling realistic feedbacks of anthropogenic climate change (Benveniste et al., 2018). Uncertainty information is often provided as a range, reflecting uncertainties related to data limitations, parameter values, and/or model structure, helping to identify the most influential model components and therefore bottlenecks in model development and outcomes (Hu et al., 2021). This information is crucial for a comprehensive understanding and comparison within the

outcomes provided by different modeling approaches. However, uncertainty evaluation techniques have often been omitted in riverine GHG models (Figure 6A). Only few publications that evaluated model uncertainties applied either Monte Carlo analysis (Rosentreter et al., 2021), error propagation (Borges et al., 2019), or generalized likelihood uncertainty estimation (Ho et al., 2021).

Large discrepancies exist in global estimates of riverine GHG emissions, however uncertainty ranges are overlooked in 56% of the cases (Figure 6B). For instance, significant discrepancies in riverine CO_2 emissions have been observed due to the inclusion of headwaters in some models (Raymond et al., 2013) and exclusion in others (Aufdenkampe et al., 2011; Lauerwald et al., 2015). Similarly, discrepancies in riverine N_2O emission estimates have been reported when incorporating headwaters (Yao et al., 2020) and hydromorphological effects in models (Marzadri et al., 2021). Furthermore, estimating global riverine CH_4 emissions remains challenging due to substantial flux variability within and between aquatic ecosystems. For instance, CH_4 empirical data distribution is skewed towards higher values making estimations sensitive to modeling assumptions and methods (Rosentreter et al., 2021). Additionally, determining surface areas of aquatic ecosystems, crucial for most riverine global models, carries significant uncertainties (Rosentreter et al., 2021; Yao et al., 2020).

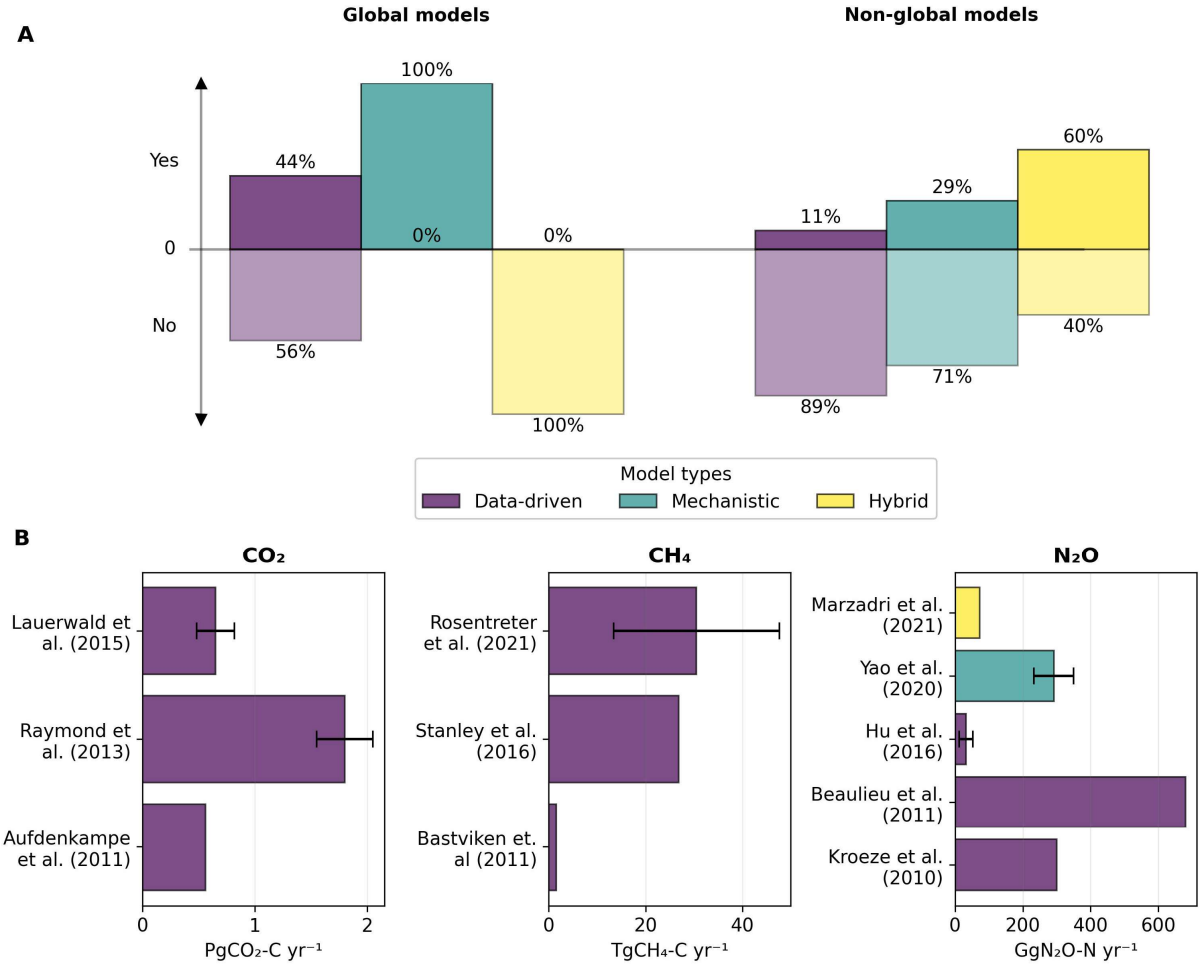

Figure 6. Application of uncertainty analysis in global and non-global riverine GHG models (A), including global estimates of riverine GHG emissions with uncertainty ranges when reported (B).

5. Application framework of riverine GHG models

Based on the characteristics of riverine GHG models, a decision tree is provided in Figure 7 to guide model selection. Specifically, model selection is based on three main criteria, including model purpose, model scale, and the spatiotemporal characteristics of GHG data. Overall, low complexity of data-driven models allows for its simple application, making these models applicable even when data is scarce. The development of more complex data-driven models, such as machine learning algorithms in GHG riverine research, is still limited by data availability. However, the use of such complex data-driven models is gradually being implemented in GHG riverine research through their combination in hybrid models, e.g., for determining catchment characteristics for global-scale predictions (Marzadri et al., 2021). Given the extensive representation of the system of mechanistic models, these can simulate temporal and spatial dynamics of GHGs being relevant for explicative or predictive purposes when sufficient spatiotemporal resolution is available to validate model outcomes. However, a fully mechanistic approach needs abundant data for large-scale applications. Then, hybrid models are particularly valuable as they can combine existent mechanistic models, such as hydrological models with a data-driven component for GHG emission calculation, therefore providing a framework suitable for combining processes occurring at different temporal and spatial scales, such as land-surface and riverine processes.

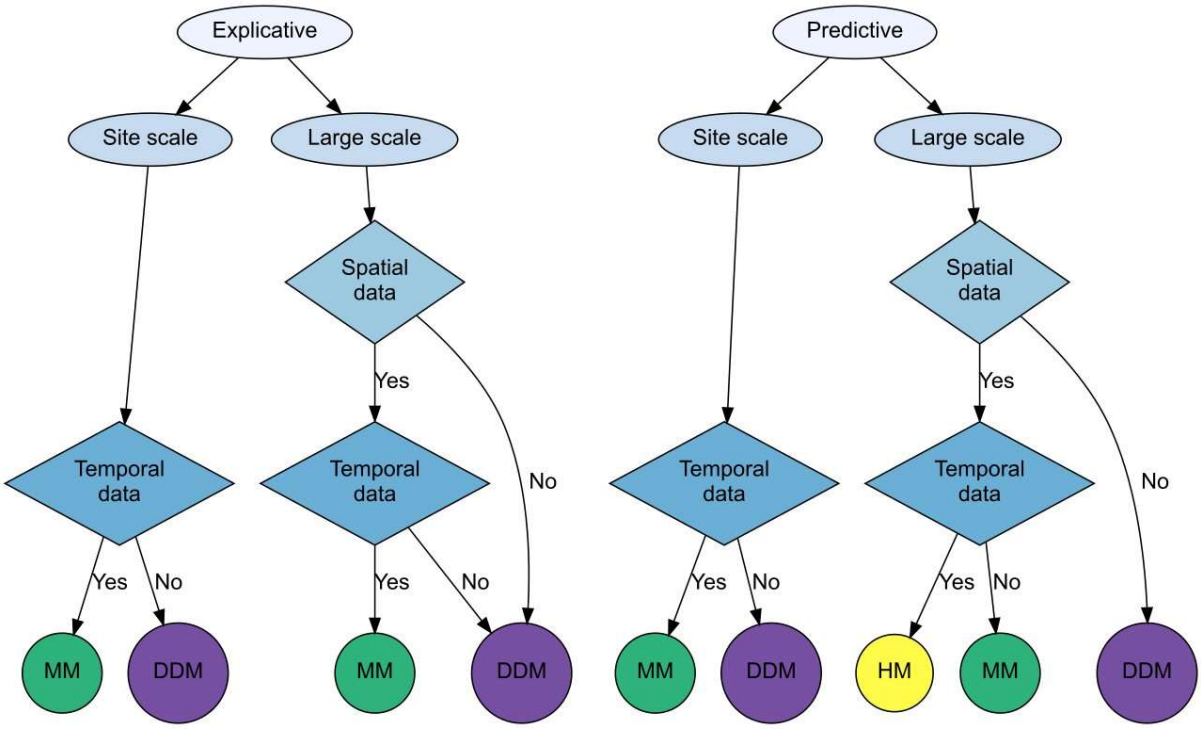

Figure 7. Decision tree for riverine GHG model selection. DDM: Data-driven models; MM: Mechanistic models; HM: Hybrid models.

6. Current challenges and future directions

After meticulously reviewing numerous research articles in multidisciplinary studies, we created a comprehensive summary outlining the factors that have restricted the advancement of riverine GHG models (Table 4). These factors are categorized into drawbacks in data availability and model development, including specific knowledge gaps described per GHG. This compilation encompasses implications and potential research directions that we strongly advocate for acknowledgment during this epoch of prolific model development.

Table 4. Main drawbacks and potential research directions for riverine GHG modeling.

Findings	Implications	Potential research directions
Drawbacks in data availability and quality		
86% of modeling studies are carried at the site scale.	- Biochemical factors are vastly studied with data-driven models, however the interplay of these local factors at larger scales is unknown. Consequently, it remains uncertain if the factors identified as significant at the site scale also apply across the entire river network.	- More basin-scale studies are needed to depict the complex interactions of in-stream biochemical factors and basin-scale LULC and geomorphological heterogeneities, together with time-dependent hydrological relationships. For this purpose, mechanistic and hybrid models are suitable, especially hybrid models that can integrate available knowledge of in-stream biochemical controls with missing basin-scale processes.
CO_2:	- Current studies fail to define relationships of riverine CO_2 evasion with basin-scale hydrological flow paths that transport DOC from organic-rich areas (e.g., croplands) and geogenic DIC to rivers (Gu et al., 2021; Liu et al., 2021; Stewart et al., 2022). Likely, transition areas from high to low slopes might support high CO_2 effluxes (Rocher-Ros et al., 2019). As such, catchment land use, geology, geomorphology and alkalinity might be relevant for predicting CO_2 emissions.	- More research is needed to explain the influence of catchment hydrology and geogenic C sources on riverine CO_2 emissions. Moreover, these factors need to be characterized and integrated into riverine GHG models, to improve scaling-up efforts and facilitate more reliable regional and global estimates.
CH_4:	- Current studies are unable to constrain river hydrological connectivity with organic-rich areas that input dissolved CH_4 (McGinnis et al., 2016; Sieczko et al., 2016; Teodoru et al., 2015), or to determine the potential effects of hydrological exchanges on CH_4 oxidation in the hyporheic zone (Villa et al., 2020). Moreover, basin geomorphology might drive patterns of sediment deposition in river channels, creating CH_4 hotspots (Sawakuchi et al., 2014).	- Researchers must apply basin models to elucidate the potential effects of hydrology and hydrodynamics in creating hotspots of CH_4 production and emissions.
N_2O:	- Catchment geology affects significantly the transport of N inputs from land surface to rivers, with low permeable aquifers	- It would be interesting to combine spatially distributed measurements of GHG fluxes and isotope analysis with hydrological

		promoting complete denitrication, whereas permeable aquifers are linked to high N_2O effluxes (Cooper et al., 2017). Additionally case studies might miss to determine the overall effect of riparian zones in regional and global reports (Billen et al., 2020; Saggar et al., 2013; Yao et al., 2020).	modeling. While flux and isotope measurements would help explain production pathways and sources (Ho et al., 2023), hydrological models would elucidate hydrological flow paths, depicting relationships between aquifer residence times and denitrification processes. This can be also applied to elucidate riparian buffer effects. The overall goal must be to characterize catchment geology, geomorphology and hydrology in order to conceptualize hyporheic and riparian denitrification rates, which are highly required for upscaling calculations.
77% of riverine GHG models are based on data collected over periods longer than a month.		- Manual measurements are vastly reported while automated measurements are missing. Consequently, datasets have low temporal resolution and are of short duration. This hampers the comprehensive investigation of factors that influence riverine GHG emissions at high temporal resolution or have long-term effects on riverine emissions. Consequently, global estimates fail to incorporate seasonal trends and elucidate feedback patterns.	- Automated and affordable data collection systems are needed. Moreover, standardized protocols and guidelines must be proposed for data collection in riverine systems which include biochemical, hydro- and geomorphological data (Ho and Goethals, 2022). This will provide compatible datasets, thereby enabling the analysis of large-scale relationships between factors, reducing data uncertainties in upscaling approaches.
	CO_2:	- Short datasets might overlook important shifts in C sources to rivers, for instance the interconnection of rivers and floodplains during high-flow periods might lead to peaks in fluxes (Gu et al., 2021; Scofield et al., 2016), whereas during low-flow periods groundwater inputs might be of great importance (Aho et al., 2021; Hotchkiss et al., 2015; Saccardi and Winnick, 2021).	- Automated measurements would generate higher GHG data resolution, which must be combined with hydrological mechanistic models to explain system flow connections and dynamics. Until these automated systems become available, researchers must prioritize experimental designs with systematic temporal measurements, including standarized protocols, with a main goal: to integrate antecedent hydrological conditions into CO_2 evasion prediction.
	CH_4:	- Current datasets fail to capture seasonal fluctuations in CH_4 emissions pathways. For instance, low-flow periods are associated with hyporheic CH_4 generation (Sawakuchi et al., 2014; Villa et al., 2020; Wang et al., 2018). Additionally, sporadic events are also missing, such as abrupt changes in water levels promoting CH_4 ebullition (Ho et al., 2021). Spatial variability in inundated and air-exposed sediments might also play an important role missing in current datasets (Bednařík et al., 2019; Villa et al., 2020).	- In addition to combining automated GHG measurements with mechanistic models to explain catchment dynamics, CH_4 models require to associate advanced remote sensing methods to include the variability of inundated-exposed river areas. As currently, advanced methods are not able to provide such data at adequate resolutions, synergies between advanced and conventional methods are needed. While advanced methods provide long-term data at large scales, yet at coarse spatiotemporal resolution (Huang et al., 2019), conventional methods offer high resolution data at site-specific locations (Wilkinson et al., 2019).
	N_2O:	- With the current GHG data resolution, the study of seasonal hydrological flow paths causing the shift in N_2O production from the hyporheic zone to the water column is incomplete (Cornejo-D'ottone et al., 2019; Hu et al., 2021; Marzadri et al., 2017). It is therefore likely that datasets might not capture important N inputs from croplands during intensive agricultural periods (Gao et al., 2020; Yao et al., 2020).	- Apart from automated measurement techniques and modeling, more isotope mixing models and mapping analysis are required to investigate potential nitrate sources to riverine systems, such as precipitation, soil N, chemical fertilizers, and manure and sewage (Barthel et al., 2022).

Drawbacks in model development		
Although data-driven models have yielded valuable insights into the dynamics of riverine GHG emissions, there is still room for improvement.	- Data-driven models mostly incorporated biochemical factors, whereas basin factors are missing. If data is limited, data-driven models have implicit difficulties to integrate spatial information (e.g., maps) with point measurements of GHGs without substantially losing information. For instance, LULC emissions, including deforestation and reforestation, are excluded in current figures of regional and global emissions. The few cases in which LULC factors are included used numerical values of percentage of the basin area, yet were unable to accurately capture the impact of LULC on riverine emissions.	- We recommend more mechanistic and hybrid models to target basin-scale simulations. Given the flexibility of hybrid models, they are able to integrate multiple drivers and data sources at diverse scales of analysis, for example, the integration of mechanistic models that simulate lateral exports from land-surface to rivers with data-driven models (existing) that simulate site-scale riverine GHG production and emissions. Such hybrid models can provide a holistic simulation of the system, especially at the basin level where the complex effects of LULC factors can be captured and models can be better constrained. Likewise, this flexibility of hybrid models makes it easy to update results when new data become available.
Large discrepancies exist within global estimates of riverine GHG emissions; yet, uncertainty ranges are overlooked in 56% of the cases.	- Overlooking uncertainty ranges hampers a comprehensive understanding of the estimates obtained from different approaches (different methodologies, assumptions, factors and data), because the potential errors, limitations and/or variability associated with each approach remain unknown.	- Incorporating uncertainty ranges must be mandatory for reporting purposes, as this facilitates more informed decision-making and helps in evaluating the robustness and effectiveness of the applied methodologies.

7. Conclusions

This review investigated the progress of riverine GHG models over the past 11 years. Three main model types have been applied: data-driven, mechanistic, and hybrid models, among which data-driven models have been predominated. These models mainly explore biochemical processes in site-scale studies, while the role of geomorphological, hydrological factors, and land use types remains largely overlooked. Limited insights and data prevent the existing models from simulating complex interaction between influencing factors, which ultimately results in uncertainties in GHG global budgets. To advance this field, we proposed an application framework for model selection in which advantages and disadvantages of the model types regarding purposes, scales, and data availability can be found. Moreover, we outlined the factors restricting model development, emphasizing the lack of basin-scale studies to explain the interplay of river-land dynamics triggering riverine GHG emissions. We highlight the need for automated data collection systems and improved experimental designs to systematically gather GHG, biochemical, hydro- and geomorphological data, to cover these knowledge gaps.

Acknowledgments

Long Ho is a postdoctoral fellow supported by the Research Foundation of Flanders (FWO) (project number 1253921N). This study is funded by the Government of Flanders through the G-STIC Climate Action Programme (IKF 21/08).

Open Research

Datasets for this research are available online at https://data.mendeley.com/datasets/2tvm63grb7/1

References

Abril, G., Bouillon, S., Darchambeau, F., Teodoru, C.R., Marwick, T.R., Tamooh, F., Ochieng Omengo, F., Geeraert, N., Deirmendjian, L., Polsenaere, P., Borges, A.V., 2015. Technical Note: Large overestimation of pCO_2 calculated from pH and alkalinity in acidic, organic-rich freshwaters. Biogeosciences 12, 67–78. https://doi.org/10.5194/bg-12-67-2015

Aho, K.S., Hosen, J.D., Logozzo, L.A., McGillis, W.R., Raymond, P.A., 2021. Highest rates of gross primary productivity maintained despite CO2 depletion in a temperate river network. Limnology And Oceanography Letters 6, 200–206. https://doi.org/10.1002/lol2.10195

Akella, C.S., Bhallamudi, S.M., 2019. Managing municipal wastewater treatment to control nitrous oxide emissions from tidal rivers. Water (Switzerland) 11. https://doi.org/10.3390/w11061255

Aufdenkampe, A.K., Mayorga, E., Raymond, P.A., Melack, J.M., Doney, S.C., Alin, S.R., Aalto, R.E., Yoo, K., 2011. Riverine coupling of biogeochemical cycles between land, oceans, and atmosphere. Frontiers in Ecology and the Environment 9, 53–60. https://doi.org/10.1890/100014

Barthel, M., Bauters, M., Baumgartner, S., Drake, T.W., Bey, N.M., Bush, G., Boeckx, P., Botefa, C.I., Dériaz, N., Ekamba, G.L., Gallarotti, N., Mbayu, F.M., Mugula, J.K., Makelele, I.A., Mbongo, C.E., Mohn, J., Mandea, J.Z., Mpambi, D.M., Ntaboba, L.C., Rukeza, M.B., Spencer, R.G.M., Summerauer, L., Vanlauwe, B., Van Oost, K., Wolf, B., Six, J., 2022. Low N2O and variable CH4 fluxes from tropical forest soils of the Congo Basin. Nature Communications 13, 330. https://doi.org/10.1038/s41467-022-27978-6

Bastviken, D., Tranvik, L.J., Downing, J.A., Crill, P.M., Enrich-Prast, A., 2011. Freshwater Methane Emissions Offset the Continental Carbon Sink. Science 331, 50–50. https://doi.org/10.1126/science.1196808

Bastviken, D., Wilk, J., Duc, N.T., Gålfalk, M., Karlson, M., Neset, T.-S., Opach, T., Enrich-Prast, A., Sundgren, I., 2022. Critical method needs in measuring greenhouse gas fluxes. Environmental Research Letters 17, 104009. https://doi.org/10.1088/1748-9326/ac8fa9

Baulch, H.M., Dillon, P.J., Maranger, R., Schiff, S.L., 2011. Diffusive and ebullitive transport of methane and nitrous oxide from streams: Are bubble-mediated fluxes important? Journal of Geophysical Research: Biogeosciences 116. https://doi.org/10.1029/2011JG001656

Beaulieu, J.J., Tank, J.L., Hamilton, S.K., Wollheim, W.M., Hall Jr., R.O., Mulholland, P.J., Peterson, B.J., Ashkenas, L.R., Cooper, L.W., Dahm, C.N., Dodds, W.K., Grimm, N.B., Johnson, S.L., McDowell, W.H., Poole, G.C., Maurice Valett, H., Arango, C.P., Bernot, M.J., Burgin, A.J., Crenshaw, C.L., Helton, A.M., Johnson, L.T., O'Brien, J.M., Potter, J.D., Sheibley, R.W., Sobota, D.J., Thomas, S.M., 2011. Nitrous oxide emission from denitrification in stream and river networks. Proceedings of the National Academy of Sciences of the United States of America 108, 214–219. https://doi.org/10.1073/pnas.1011464108

Bednařík, A., Blaser, M., RuLíK, M., 2019. Methane formation and consumption by sediments in a cross-channel profile of a small river impoundment. Journal of Limnology 78.

Begum, M.S., Bogard, M.J., Butman, D.E., Chea, E., Kumar, S., Lu, X., Nayna, O.K., Ran, L., Richey, J.E., Tareq, S.M., Xuan, D.T., Yu, R., Park, J.-H., 2021. Localized Pollution Impacts on Greenhouse Gas Dynamics in Three Anthropogenically Modified Asian River Systems. Journal of Geophysical Research: Biogeosciences 126. https://doi.org/10.1029/2020JG006124

Benveniste, H., Boucher, O., Guivarch, C., Treut, H.L., Criqui, P., 2018. Impacts of nationally determined contributions on 2030 global greenhouse gas emissions: uncertainty analysis and distribution of emissions. Environmental Research Letters 13, 014022. https://doi.org/10.1088/1748-9326/aaa0b9

Billen, G., Garnier, J., Grossel, A., Thieu, V., Théry, S., Hénault, C., 2020. Modeling indirect N2O emissions along the N cascade from cropland soils to rivers. Biogeochemistry 148, 207–221. https://doi.org/10.1007/s10533-020-00654-x

Borges, A.V., Darchambeau, F., Lambert, T., Morana, C., Allen, G.H., Tambwe, E., Toengaho Sembaito, A., Mambo, T., Wabakhangazi, J.N., Descy, J.-P., Teodoru, C.R., Bouillon, S., 2019. Variations in dissolved greenhouse gases (CO2, CH4, N2O) in the Congo River network overwhelmingly driven by fluvial-wetland connectivity. Biogeosciences 16, 3801–3834. https://doi.org/10.5194/bg-16-3801-2019

562 Borges, A.V., Darchambeau, F., Teodoru, C.R., Marwick, T.R., Tamooh, F., Geeraert, N., Omengo,
563 F.O., Guérin, F., Lambert, T., Morana, C., Okuku, E., Bouillon, S., 2015. Globally significant
564 greenhouse-gas emissions from African inland waters. Nature Geoscience 8, 637–642.
565 https://doi.org/10.1038/ngeo2486
566 Campeau, A., Del Giorgio, P.A., 2014. Patterns in CH4 and CO2 concentrations across boreal rivers:
567 Major drivers and implications for fluvial greenhouse emissions under climate change
568 scenarios. Global Change Biology 20, 1075–1088. https://doi.org/10.1111/gcb.12479
569 Chen, V., Li, J., Kim, J.S., Plumb, G., Talwalkar, A., 2022. Interpretable Machine Learning: Moving
570 from mythos to diagnostics. Queue 19, Pages 10:28-Pages 10:56.
571 https://doi.org/10.1145/3511299
572 Cole, J.J., Prairie, Y.T., Caraco, N.F., McDowell, W.H., Tranvik, L.J., Striegl, R.G., Duarte, C.M.,
573 Kortelainen, P., Downing, J.A., Middelburg, J.J., Melack, J., 2007. Plumbing the Global
574 Carbon Cycle: Integrating Inland Waters into the Terrestrial Carbon Budget. Ecosystems 10,
575 172–185. https://doi.org/10.1007/s10021-006-9013-8
576 Cooper, R.J., Wexler, S.K., Adams, C.A., Hiscock, K.M., 2017. Hydrogeological Controls on
577 Regional-Scale Indirect Nitrous Oxide Emission Factors for Rivers. Environmental Science
578 and Technology 51, 10440–10448. https://doi.org/10.1021/acs.est.7b02135
579 Cornejo-D'ottone, M., Figueroa, R., Parra, O., 2019. Seasonality of the N2O cycle of the biobío river
580 during the megadrought. Journal of Limnology 78, 14–26.
581 https://doi.org/10.4081/jlimnol.2018.1767
582 Drake, T.W., Raymond, P.A., Spencer, R.G.M., 2018. Terrestrial carbon inputs to inland waters: A
583 current synthesis of estimates and uncertainty. Limnology and Oceanography Letters 3, 132–
584 142. https://doi.org/10.1002/lol2.10055
585 Gao, X., Ouyang, W., Lin, C., Wang, K., Hao, F., Hao, X., Lian, Z., 2020. Considering atmospheric
586 N2O dynamic in SWAT model avoids the overestimation of N2O emissions in river
587 networks. Water Research 174. https://doi.org/10.1016/j.watres.2020.115624
588 Gu, C., Waldron, S., Bass, A.M., 2021. Carbon dioxide, methane, and dissolved carbon dynamics in
589 an urbanized river system. Hydrological Processes 35, e14360.
590 https://doi.org/10.1002/hyp.14360
591 Hall Jr., R.O., Ulseth, A.J., 2020. Gas exchange in streams and rivers. WIREs Water 7, e1391.
592 https://doi.org/10.1002/wat2.1391
593 Hao, X., Ruihong, Y., Zhuangzhuang, Z., Zhen, Q., Xixi, L., Tingxi, L., Ruizhong, G., 2021.
594 Greenhouse gas emissions from the water–air interface of a grassland river: a case study of
595 the Xilin River. Scientific Reports 11. https://doi.org/10.1038/s41598-021-81658-x
596 Ho, L., Barthel, M., Harris, S., Vermeulen, K., Six, J., Bodé, S., Boeckx, P., Goethals, P., 2023.
597 Unravelling spatiotemporal N2O dynamics in an urbanized estuary system using natural
598 abundance isotopes. Water Research 247, 120771.
599 https://doi.org/10.1016/j.watres.2023.120771
600 Ho, L., Goethals, P., 2022. Machine learning applications in river research: Trends, opportunities and
601 challenges. Methods in Ecology and Evolution 13, 2603–2621. https://doi.org/10.1111/2041-
602 210X.13992
603 Ho, L., Jerves-Cobo, R., Eurie Forio, M.A., Mouton, A., Nopens, I., Goethals, P., 2021. Integrated
604 mechanistic and data-driven modeling for risk assessment of greenhouse gas production in an
605 urbanized river system. Journal of Environmental Management 294.
606 https://doi.org/10.1016/j.jenvman.2021.112999
607 Ho, L.T., Alvarado, A., Larriva, J., Pompeu, C., Goethals, P., 2019. An integrated mechanistic
608 modeling of a facultative pond: Parameter estimation and uncertainty analysis. Water
609 Research 151, 170–182. https://doi.org/10.1016/j.watres.2018.12.018
610 Hotchkiss, E.R., Hall Jr, R.O., Sponseller, R.A., Butman, D., Klaminder, J., Laudon, H., Rosvall, M.,
611 Karlsson, J., 2015. Sources of and processes controlling CO2emissions change with the size
612 of streams and rivers. Nature Geoscience 8, 696–699. https://doi.org/10.1038/ngeo2507
613 Hu, M., Chen, D., Dahlgren, R.A., 2016. Modeling nitrous oxide emission from rivers: a global
614 assessment. Global Change Biology 22, 3566–3582. https://doi.org/10.1111/gcb.13351

Hu, M., Li, B., Wu, K., Zhang, Y., Wu, H., Zhou, J., Chen, D., 2021. Modeling Riverine N2O Sources, Fates, and Emission Factors in a Typical River Network of Eastern China. Environ. Sci. Technol. 55, 13356–13365. https://doi.org/10.1021/acs.est.1c01301

Huang, W., Xiao, W., Zhang, M., Wang, W., Xu, J., Hu, Y., Hu, C., Liu, S., Lee, X., 2019. Anthropogenic CH4 emissions in the Yangtze River Delta based on a "top-down" method. Atmosphere 10. https://doi.org/10.3390/atmos10040185

Hunt, C.W., Salisbury, J.E., Vandemark, D., 2011. Contribution of non-carbonate anions to total alkalinity and overestimation of pCO_2 in New England and New Brunswick rivers. Biogeosciences 8, 3069–3076. https://doi.org/10.5194/bg-8-3069-2011

Ion, I.V., Ene, A., 2021. Evaluation of Greenhouse Gas Emissions from Reservoirs: A Review. Sustainability 13, 11621. https://doi.org/10.3390/su132111621

IPCC, 2019. 2019 Refinement to the 2006 IPCC Guidelines for National Greenhouse Gas Inventories, Calvo Buendia, E., Tanabe, K., Kranjc, A., Baasansuren, J., Fukuda, M., Ngarize, S., Osako, A., Pyrozhenko, Y., Shermanau, P. and Federici, S. (eds). IPCC, Switzerland.

IPCC, 2006. 2006 IPCC Guidelines for National Greenhouse Gas Inventories. Prepared by the National Greenhouse Gas Inventories Programme, Eggleston H.S., Buendia L., Miwa K., Ngara T. and Tanabe K. (eds). IGES, Japan.

Jia, X., Zwart, J., Sadler, J., Appling, A., Oliver, S., Markstrom, S., Willard, J., Xu, S., Steinbach, M., Read, J., Kumar, V., 2020. Physics-Guided Recurrent Graph Networks for Predicting Flow and Temperature in River Networks. https://doi.org/10.48550/arXiv.2009.12575

Johnson, M.S., Billett, M.F., Dinsmore, K.J., Wallin, M., Dyson, K.E., Jassal, R.S., 2010. Direct and continuous measurement of dissolved carbon dioxide in freshwater aquatic systems—method and applications. Ecohydrology 3, 68–78. https://doi.org/10.1002/eco.95

Keenan, T.F., Williams, C.A., 2018. The Terrestrial Carbon Sink. Annual Review of Environment and Resources 43, 219–243. https://doi.org/10.1146/annurev-environ-102017-030204

Kratzert, F., Herrnegger, M., Klotz, D., Hochreiter, S., Klambauer, G., 2019. NeuralHydrology – Interpreting LSTMs in Hydrology. pp. 347–362. https://doi.org/10.1007/978-3-030-28954-6_19

Lauerwald, R., Allen, G.H., Deemer, B.R., Liu, S., Maavara, T., Raymond, P., Alcott, L., Bastviken, D., Hastie, A., Holgerson, M.A., Johnson, M.S., Lehner, B., Lin, P., Marzadri, A., Ran, L., Tian, H., Yang, X., Yao, Y., Regnier, P., 2023. Inland Water Greenhouse Gas Budgets for RECCAP2: 1. State-Of-The-Art of Global Scale Assessments. Global Biogeochemical Cycles 37, e2022GB007657. https://doi.org/10.1029/2022GB007657

Lauerwald, R., Laruelle, G.G., Hartmann, J., Ciais, P., Regnier, P.A.G., 2015. Spatial patterns in CO2 evasion from the global river network. Global Biogeochemical Cycles 29, 534–554. https://doi.org/10.1002/2014GB004941

Levasseur, A., Mercier-Blais, S., Prairie, Y.T., Tremblay, A., Turpin, C., 2021. Improving the accuracy of electricity carbon footprint: Estimation of hydroelectric reservoir greenhouse gas emissions. Renewable and Sustainable Energy Reviews 136, 110433. https://doi.org/10.1016/j.rser.2020.110433

Lewis, E.R., Wallace, D.W.R., 1998. Program Developed for CO2 System Calculations (No. cdiac:CDIAC-105). Environmental System Science Data Infrastructure for a Virtual Ecosystem (ESS-DIVE) (United States). https://doi.org/10.15485/1464255

Li, S., Lu, X.X., Bush, R.T., 2013. CO2 partial pressure and CO2 emission in the Lower Mekong River. Journal of Hydrology 504, 40–56. https://doi.org/10.1016/j.jhydrol.2013.09.024

Liu, B., Tian, M., Shih, K., Chan, C.N., Yang, X., Ran, L., 2021. Spatial and temporal variability of pCO2 and CO2 emissions from the Dong River in south China. Biogeosciences 18, 5231–5245. https://doi.org/10.5194/bg-18-5231-2021

Liu, S., Butman, D.E., Raymond, P.A., 2020. Evaluating CO2 calculation error from organic alkalinity and pH measurement error in low ionic strength freshwaters. Limnology and Oceanography: Methods 18, 606–622. https://doi.org/10.1002/lom3.10388

Liu, S., Kuhn, C., Amatulli, G., Aho, K., Butman, D.E., Allen, G.H., Lin, P., Pan, M., Yamazaki, D., Brinkerhoff, C., Gleason, C., Xia, X., Raymond, P.A., 2022. The importance of hydrology in routing terrestrial carbon to the atmosphere via global streams and rivers. Proceedings of the National Academy of Sciences 119, e2106322119. https://doi.org/10.1073/pnas.2106322119

Mallast, U., Staniek, M., Koschorreck, M., 2020. Spatial upscaling of CO2 emissions from exposed river sediments of the Elbe River during an extreme drought. Ecohydrology 13. https://doi.org/10.1002/eco.2216

Manning, C.C., Preston, V.L., Jones, S.F., Michel, A.P.M., Nicholson, D.P., Duke, P.J., Ahmed, M.M.M., Manganini, K., Else, B.G.T., Tortell, P.D., 2020. River Inflow Dominates Methane Emissions in an Arctic Coastal System. Geophysical Research Letters 47, e2020GL087669. https://doi.org/10.1029/2020GL087669

Marzadri, A., Amatulli, G., Tonina, D., Bellin, A., Shen, L.Q., Allen, G.H., Raymond, P.A., 2021. Global riverine nitrous oxide emissions: The role of small streams and large rivers. Science of The Total Environment 776, 145148. https://doi.org/10.1016/j.scitotenv.2021.145148

Marzadri, A., Dee, M.M., Tonina, D., Bellin, A., Tank, J.L., 2017. Role of surface and subsurface processes in scaling N2O emissions along riverine networks. Proceedings of the National Academy of Sciences of the United States of America 114, 4330–4335. https://doi.org/10.1073/pnas.1617454114

Marzadri, A., Tonina, D., Bellin, A., 2020. Power law scaling model predicts N2O emissions along the Upper Mississippi River basin. Science of The Total Environment 732, 138390. https://doi.org/10.1016/j.scitotenv.2020.138390

McGinnis, D.F., Bilsley, N., Schmidt, M., Fietzek, P., Bodmer, P., Premke, K., Lorke, A., Flury, S., 2016. Deconstructing Methane Emissions from a Small Northern European River: Hydrodynamics and Temperature as Key Drivers. Environmental Science and Technology 50, 11680–11687. https://doi.org/10.1021/acs.est.6b03268

Mishima, I., Masuda, S., Kakimoto, T., Ikeda, K., Watanabe, K., Maruo, C., Nishimura, O., 2021. Assessment of nitrous oxide production in eutrophicated rivers with inflow of treated wastewater based on investigation and statistical analysis. Environ Monit Assess 193, 93. https://doi.org/10.1007/s10661-021-08855-z

Morozumi, T., Shingubara, R., Murase, J., Nagai, S., Kobayashi, H., Takano, S., Tei, S., Fan, R., Maximov, T.C., Sugimoto, A., 2019. Usability of water surface reflectance for the determination of riverine dissolved methane during extreme flooding in northeastern Siberia. Polar Science 21, 186–194. https://doi.org/10.1016/j.polar.2019.01.005

Mwanake, R.M., Gettel, G.M., Aho, K.S., Namwaya, D.W., Masese, F.O., Butterbach-Bahl, K., Raymond, P.A., 2019. Land Use, Not Stream Order, Controls N2O Concentration and Flux in the Upper Mara River Basin, Kenya. Journal of Geophysical Research: Biogeosciences 124, 3491–3506. https://doi.org/10.1029/2019JG005063

Newcomer, M.E., Hubbard, S.S., Fleckenstein, J.H., Maier, U., Schmidt, C., Thullner, M., Ulrich, C., Flipo, N., Rubin, Y., 2018. Influence of Hydrological Perturbations and Riverbed Sediment Characteristics on Hyporheic Zone Respiration of CO2 and N2. Journal of Geophysical Research: Biogeosciences 123, 902–922. https://doi.org/10.1002/2017JG004090

Nordstrom, D.K., Plummer, L.N., Wigley, T.M.L., Wolery, T.J., Ball, J.W., Jenne, E.A., Bassett, R.L., Crerar, D.A., Florence, T.M., Fritz, B., Hoffmann, M., Holdren, G.R., Lafon, G.M., Mattigod, S.V., McDuff, R.E., Morel, F., Reddy, M.M., Sposito, G., Thrailkill, J., 1979. A Comparison of Computerized Chemical Models for Equilibrium Calculations in Aqueous Systems, in: Jenne, Everett Arthur (Ed.), . Presented at the 176th Meeting of the American Chemical Society, American Chemical Society, Washington, DC, pp. 857–892.

Palmer, P.I., O'Doherty, S., Allen, G., Bower, K., Bösch, H., Chipperfield, M.P., Connors, S., Dhomse, S., Feng, L., Finch, D.P., Gallagher, M.W., Gloor, E., Gonzi, S., Harris, N.R.P., Helfter, C., Humpage, N., Kerridge, B., Knappett, D., Jones, R.L., Le Breton, M., Lunt, M.F., Manning, A.J., Matthiesen, S., Muller, J.B.A., Mullinger, N., Nemitz, E., O'Shea, S., Parker, R.J., Percival, C.J., Pitt, J., Riddick, S.N., Rigby, M., Sembhi, H., Siddans, R., Skelton, R.L., Smith, P., Sonderfeld, H., Stanley, K., Stavert, A.R., Wenger, A., White, E., Wilson, C., Young, D., 2018. A measurement-based verification framework for UK greenhouse gas emissions: an overview of the Greenhouse gAs Uk and Global Emissions (GAUGE) project. Atmospheric Chemistry and Physics 18, 11753–11777. https://doi.org/10.5194/acp-18-11753-2018

Parkhurst, D., Appelo, C., 2013. Description of input and examples for PHREEQC version 3: a computer program for speciation, batch-reaction, one-dimensional transport, and inverse geochemical calculations.

Pfeiffer-Herbert, A.S., Prahl, F.G., Hales, B., Lerczak, J.A., Pierce, S.D., Levine, M.D., 2016. High resolution sampling of methane transport in the Columbia River near-field plume: Implications for sources and sinks in a river-dominated estuary. Limnology and Oceanography 61, S204–S220. https://doi.org/10.1002/lno.10221

Pfeiffer-Herbert, A.S., Prahl, F.G., Peterson, T.D., Wolhowe, M., 2019. Methane Dynamics Associated with Tidal Processes in the Lower Columbia River. Estuaries and Coasts 42, 1249–1264. https://doi.org/10.1007/s12237-019-00568-4

Quick, A.M., Reeder, W.J., Farrell, T.B., Tonina, D., Feris, K.P., Benner, S.G., 2019. Nitrous oxide from streams and rivers: A review of primary biogeochemical pathways and environmental variables. Earth-Science Reviews 191, 224–262. https://doi.org/10.1016/j.earscirev.2019.02.021

Ran, L., Shi, H., Yang, X., 2021. Magnitude and drivers of CO2 and CH4 emissions from an arid/semiarid river catchment on the Chinese Loess Plateau. Journal of Hydrology 598. https://doi.org/10.1016/j.jhydrol.2021.126260

Raymond, P.A., Hartmann, J., Lauerwald, R., Sobek, S., McDonald, C., Hoover, M., Butman, D., Striegl, R., Mayorga, E., Humborg, C., Kortelainen, P., Dürr, H., Meybeck, M., Ciais, P., Guth, P., 2013. Global carbon dioxide emissions from inland waters. Nature 503, 355–359. https://doi.org/10.1038/nature12760

Rocher-Ros, G., Sponseller, R.A., Lidberg, W., Mörth, C.-M., Giesler, R., 2019. Landscape process domains drive patterns of CO2 evasion from river networks. Limnology and Oceanography Letters 4, 87–95. https://doi.org/10.1002/lol2.10108

Rosentreter, J.A., Borges, A.V., Deemer, B.R., Holgerson, M.A., Liu, S., Song, C., Melack, J., Raymond, P.A., Duarte, C.M., Allen, G.H., Olefeldt, D., Poulter, B., Battin, T.I., Eyre, B.D., 2021. Half of global methane emissions come from highly variable aquatic ecosystem sources. Nat. Geosci. 14, 225–230. https://doi.org/10.1038/s41561-021-00715-2

Saccardi, B., Winnick, M., 2021. Improving Predictions of Stream CO2 Concentrations and Fluxes Using a Stream Network Model: A Case Study in the East River Watershed, CO, USA. Global Biogeochemical Cycles 35. https://doi.org/10.1029/2021GB006972

Saggar, S., Jha, N., Deslippe, J., Bolan, N.S., Luo, J., Giltrap, D.L., Kim, D.-G., Zaman, M., Tillman, R.W., 2013. Denitrification and N2O:N2 production in temperate grasslands: Processes, measurements, modelling and mitigating negative impacts. Science of The Total Environment, Soil as a Source & Sink for Greenhouse Gases 465, 173–195. https://doi.org/10.1016/j.scitotenv.2012.11.050

Sawakuchi, H.O., Bastviken, D., Sawakuchi, A.O., Krusche, A.V., Ballester, M.V.R., Richey, J.E., 2014. Methane emissions from Amazonian Rivers and their contribution to the global methane budget. Global Change Biology 20, 2829–2840. https://doi.org/10.1111/gcb.12646

Schneider, M.Y., Quaghebeur, W., Borzooei, S., Froemelt, A., Li, F., Saagi, R., Wade, M.J., Zhu, J.-J., Torfs, E., 2022. Hybrid modelling of water resource recovery facilities: status and opportunities. Water Science and Technology 85, 2503–2524. https://doi.org/10.2166/wst.2022.115

Scofield, V., Melack, J.M., Barbosa, P.M., Amaral, J.H.F., Forsberg, B.R., Farjalla, V.F., 2016. Carbon dioxide outgassing from Amazonian aquatic ecosystems in the Negro River basin. Biogeochemistry 129, 77–91. https://doi.org/10.1007/s10533-016-0220-x

Seitzinger, S.P., Kroeze, C., 1998. Global distribution of nitrous oxide production and N inputs in freshwater and coastal marine ecosystems. Global Biogeochemical Cycles 12, 93–113. https://doi.org/10.1029/97GB03657

Shen, X., Su, M., Sun, T., Lv, S., Dang, Z., Yang, Z., 2020. Net heterotrophy and low carbon dioxide emissions from biological processes in the Yellow River Estuary, China. Water Research 171. https://doi.org/10.1016/j.watres.2019.115457

Sieczko, A.K., Demeter, K., Singer, G.A., Tritthart, M., Preiner, S., Mayr, M., Meisterl, K., Peduzzi, P., 2016. Aquatic methane dynamics in a human-impacted river-floodplain of the Danube. Limnology and Oceanography 61, S175–S187. https://doi.org/10.1002/lno.10346

Stanley, E.H., Casson, N.J., Christel, S.T., Crawford, J.T., Loken, L.C., Oliver, S.K., 2016. The ecology of methane in streams and rivers: Patterns, controls, and global significance. Ecological Monographs 86, 146–171. https://doi.org/10.1890/15-1027

Stets, E.G., Butman, D., McDonald, C.P., Stackpoole, S.M., DeGrandpre, M.D., Striegl, R.G., 2017. Carbonate buffering and metabolic controls on carbon dioxide in rivers. Global Biogeochemical Cycles 31, 663–677. https://doi.org/10.1002/2016GB005578

Stewart, B., Zhi, W., Sadayappan, K., Sterle, G., Harpold, A., Li, L., 2022. Soil CO2 Controls Short-Term Variation but Climate Regulates Long-Term Mean of Riverine Inorganic Carbon. Global Biogeochemical Cycles 36, e2022GB007351. https://doi.org/10.1029/2022GB007351

Tang, Wei, Jun Xu, Y., Li, S., 2021. Rapid urbanization effects on partial pressure and emission of CO2 in three rivers with different urban intensities. Ecological Indicators 125, 107515. https://doi.org/10.1016/j.ecolind.2021.107515

Tang, W., Xu, Y.J., Ma, Y., Maher, D.T., Li, S., 2021. Hot spot of CH4 production and diffusive flux in rivers with high urbanization. Water Research 204. https://doi.org/10.1016/j.watres.2021.117624

Teodoru, C.R., Nyoni, F.C., Borges, A.V., Darchambeau, F., Nyambe, I., Bouillon, S., 2015. Dynamics of greenhouse gases (CO_2, CH_4, N_2O) along the Zambezi River and major tributaries, and their importance in the riverine carbon budget. Biogeosciences 12, 2431–2453. https://doi.org/10.5194/bg-12-2431-2015

Thanh Duc, N., Silverstein, S., Wik, M., Crill, P., Bastviken, D., Varner, R.K., 2020. Technical note: Greenhouse gas flux studies: an automated online system for gas emission measurements in aquatic environments. Hydrology and Earth System Sciences 24, 3417–3430. https://doi.org/10.5194/hess-24-3417-2020

Thorpe, A.K., Frankenberg, C., Thompson, D.R., Duren, R.M., Aubrey, A.D., Bue, B.D., Green, R.O., Gerilowski, K., Krings, T., Borchardt, J., Kort, E.A., Sweeney, C., Conley, S., Roberts, D.A., Dennison, P.E., 2017. Airborne DOAS retrievals of methane, carbon dioxide, and water vapor concentrations at high spatial resolution: application to AVIRIS-NG. Atmospheric Measurement Techniques 10, 3833–3850. https://doi.org/10.5194/amt-10-3833-2017

Tian, H., Xu, R., Canadell, J.G., Thompson, R.L., Winiwarter, W., Suntharalingam, P., Davidson, E.A., Ciais, P., Jackson, R.B., Janssens-Maenhout, G., Prather, M.J., Regnier, P., Pan, N., Pan, S., Peters, G.P., Shi, H., Tubiello, F.N., Zaehle, S., Zhou, F., Arneth, A., Battaglia, G., Berthet, S., Bopp, L., Bouwman, A.F., Buitenhuis, E.T., Chang, J., Chipperfield, M.P., Dangal, S.R.S., Dlugokencky, E., Elkins, J.W., Eyre, B.D., Fu, B., Hall, B., Ito, A., Joos, F., Krummel, P.B., Landolfi, A., Laruelle, G.G., Lauerwald, R., Li, W., Lienert, S., Maavara, T., MacLeod, M., Millet, D.B., Olin, S., Patra, P.K., Prinn, R.G., Raymond, P.A., Ruiz, D.J., van der Werf, G.R., Vuichard, N., Wang, J., Weiss, R.F., Wells, K.C., Wilson, C., Yang, J., Yao, Y., 2020. A comprehensive quantification of global nitrous oxide sources and sinks. Nature 586, 248–256. https://doi.org/10.1038/s41586-020-2780-0

Tonina, D., Marzadri, A., Bellin, A., Dee, M.M., Bernal, S., Tank, J.L., 2021. Nitrous Oxide Emissions From Drying Streams and Rivers. Geophysical Research Letters 48. https://doi.org/10.1029/2021GL095305

Valerio, A.M., Kampel, M., Ward, N.D., Sawakuchi, H.O., Cunha, A.C., Richey, J.E., 2021. CO2 partial pressure and fluxes in the Amazon River plume using in situ and remote sensing data. Continental Shelf Research 215, 104348. https://doi.org/10.1016/j.csr.2021.104348

Vanderborght, J.P., Wollast, R., Loijens, M., Regnier, P., 2002. Application of a transport-reaction model to the estimation of biogas fluxes in the Scheldt estuary. Biogeochemistry 59, 207–237. https://doi.org/10.1023/A:1015573131561

Villa, J.A., Smith, G.J., Ju, Y., Renteria, L., Angle, J.C., Arntzen, E., Harding, S.F., Ren, H., Chen, X., Sawyer, A.H., Graham, E.B., Stegen, J.C., Wrighton, K.C., Bohrer, G., 2020. Methane and nitrous oxide porewater concentrations and surface fluxes of a regulated river. Science of the Total Environment 715. https://doi.org/10.1016/j.scitotenv.2020.136920

Wang, R., Zhang, H., Zhang, W., Zheng, X., Butterbach-Bahl, K., Li, S., Han, S., 2020. An urban polluted river as a significant hotspot for water–atmosphere exchange of CH4 and N2O. Environmental Pollution 264. https://doi.org/10.1016/j.envpol.2020.114770

Wang, X., He, Y., Chen, H., Yuan, X., Peng, C., Yue, J., Zhang, Q., Zhou, L., 2018. CH4 concentrations and fluxes in a subtropical metropolitan river network: Watershed urbanization impacts and environmental controls. Science of the Total Environment 622–623, 1079–1089. https://doi.org/10.1016/j.scitotenv.2017.12.054

Wilkinson, J., Bodmer, P., Lorke, A., 2019. Methane dynamics and thermal response in impoundments of the Rhine River, Germany. Science of The Total Environment 659, 1045–1057. https://doi.org/10.1016/j.scitotenv.2018.12.424

Wilkinson, J., Maeck, A., Alshboul, Z., Lorke, A., 2015. Continuous Seasonal River Ebullition Measurements Linked to Sediment Methane Formation. Environmental Science and Technology 49, 13121–13129. https://doi.org/10.1021/acs.est.5b01525

Willard, J., Jia, X., Xu, S., Steinbach, M., Kumar, V., 2020. Integrating physics-based modeling with machine learning: A survey. arXiv preprint arXiv:2003.04919 1, 1–34.

Xia, Y., She, D., Li, Y., Yan, X., 2014. Impact of sampling time on chamber-based measurements of riverine nitrous oxide emissions using relative difference analysis. Geoderma 214–215, 197–203. https://doi.org/10.1016/j.geoderma.2013.09.011

Xiao, Q., Hu, Z., Hu, C., Islam, A.R.M.T., Bian, H., Chen, S., Liu, C., Lee, X., 2021. A highly agricultural river network in Jurong Reservoir watershed as significant CO2 and CH4 sources. Science of the Total Environment 769. https://doi.org/10.1016/j.scitotenv.2020.144558

Yan, W., Yang, L., Wang, F., Wang, J., Ma, P., 2012. Riverine N2O concentrations, exports to estuary and emissions to atmosphere from the Changjiang River in response to increasing nitrogen loads. Global Biogeochemical Cycles 26. https://doi.org/10.1029/2010GB003984

Yang, P., Luo, L., Tang, K.W., Lai, D.Y.F., Tong, C., Hong, Y., Zhang, L., 2022. Environmental drivers of nitrous oxide emission factor for a coastal reservoir and its catchment areas in southeastern China. Environmental Pollution 294, 118568. https://doi.org/10.1016/j.envpol.2021.118568

Yang, S., Chen, I.C., Liu, C., Liu, L., Chang, C., 2015. Carbon dioxide and methane emissions from Tanswei River in Northern Taiwan. Atmospheric Pollution Research 6, 52–61. https://doi.org/10.5094/APR.2015.007

Yao, Y., Tian, H., Shi, H., Pan, S., Xu, R., Pan, N., Canadell, J.G., 2020. Increased global nitrous oxide emissions from streams and rivers in the Anthropocene. Nat. Clim. Chang. 10, 138–142. https://doi.org/10.1038/s41558-019-0665-8

Zhang, T., Li, J., Pu, J., Martin, J.B., Wang, S., Yuan, D., 2020. Rainfall possibly disturbs the diurnal pattern of CO2 degassing in the Lijiang River, SW China. Journal of Hydrology 590, 125540. https://doi.org/10.1016/j.jhydrol.2020.125540